Chapter 7

ELECTRONIC SPECTRA OF CONJUGATED POLYMERS AND OLIGOMERS

Yukio Furukawa

Department of Chemistry, School of Science and Engineering, Waseda University, Shinjuku-ku, Tokyo 169-8555, Japan

Contents

1. INTRODUCTION

The science and technology of conjugated conducting polymers have advanced very rapidly since the first report of metallic conductivities in doped polyacetylene in 1977 [1]. Following the case of polyacetylene, other conducting polymers, such as polypyrrole, polythiophene, poly(*p*-phenylene), polyaniline, poly(*p*-phenylenevinylene), and poly(2,5-thienylenevinylene), have been reported. The chemical structures of conjugated polymers are shown in Figure 1. They have a variety of chemical moieties such as the vinylene group, benzene rings, and heterocycles. A large number of studies published during the past 23 years have opened a new field in materials science that encompasses solid-state and theoretical physics, synthetic chemistry, and device engineering [2, 3]. Although conjugated polymers have been developed as organic conductors, they can be used for semiconductor devices instead of inorganic materials. Semiconductor devices fabricated with conjugated polymers, such as transistors [4, 5], photodiodes [6], and light-emitting diodes [7], have been proposed. Conjugated polymers with various substituents such as long alkyl chains are soluble in organic solvents. Since soluble and high-purity polymers became available, polymer semiconductor devices have been developed extensively [8–10]. Conjugated oligomers have been investigated as models of conjugated polymers, whereas they themselves have potential applications in electronic devices. Novel properties of con-

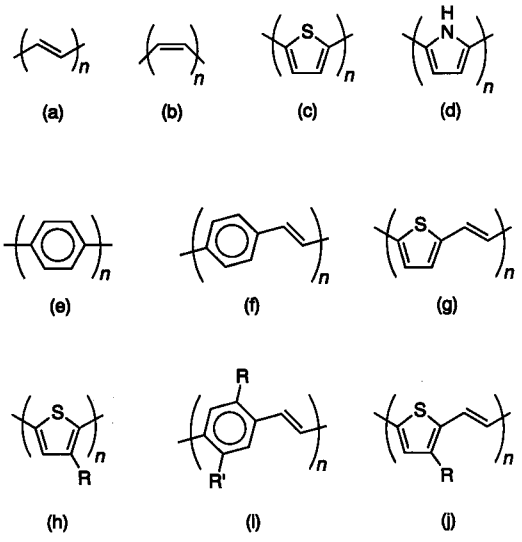

Fig. 1. Chemical structures of conjugated polymers: (a) *trans*-polyacetylene; (b) *cis*-polyacetylene; (c) polythiophene; (d) polypyrrole; (e) poly(*p*-phenylene); (f) poly(*p*-phenylenevinylene); (g) poly(2,5-thienylenevinylene); (h) substituted polythiophenes (R: H, C_6H_{13}, C_8H_{17}, $C_{10}H_{21}$, $C_{12}H_{25}$, etc.); (i) substituted poly(*p*-phenylenevinylene)s (R, R′: H, OCH_3, OC_6H_{13}, OC_8H_{17}, etc.); (j) substituted poly(2,5-thienylenevinylene)s (R: H, C_4H_9, etc.).

Handbook of Advanced Electronic and Photonic Materials and Devices, edited by H.S. Nalwa
Volume 8: Conducting Polymers

ISBN 0-12-513758-3/$35.00

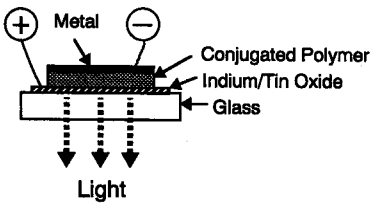

Fig. 2. Schematic structure of a light-emitting diode fabricated with a conjugated polymer.

jugated systems originate from π-electrons that respond easily to external electric and magnetic fields.

Most of the undoped conjugated polymers are organic semiconductors. Optical bandgaps of conjugated polymers are in the range from 1 to 3 eV [11]. When a conjugated polymer is irradiated by light across its bandgap, charge separation occurs. The charge separation can result in the formation of charge carriers and the polymer shows photoconductivity. Upon the addition of an electron acceptor such as C_{60}, photoconductivity is enhanced dramatically [12]. Thus, conjugated polymer–C_{60} composites are good active layers for photovoltaic devices such as photodetectors or solar cells. Electroluminescence, the generation of light by electrical excitation, is observed for organic materials. Conjugated polymers can be used for active layers in electroluminescent devices (light-emitting diodes). The schematic structure of a one-layer light-emitting diode fabricated with a conjugated polymer is shown in Figure 2. Spreitzer et al. [13] recently reported that light-emitting diodes fabricated with a copolymer of poly(*p*-phenylenevinylene) derivatives show very high power efficiency (16 lm/W); this value is comparable to that of light-emitting diodes fabricated with inorganic semiconductors or organic molecules. The process response for electroluminescence requires injection of electrons from one electrode and holes from the other, the capture of oppositely charged carriers (so-called recombination), and the radiative decay of the excited electron–hole state (exciton) produced by this recombination process.

Chemical doping is performed by exposing a polymer film in various ways to an electron acceptor (iodine, AsF_5, H_2SO_4, etc.) or an electron donor (alkali metals, etc.). The main process of doping is a redox reaction between polymer chains and acceptors or donors. Upon acceptor doping (p-type doping), an ionic complex that consists of positively charged polymer chains and counteranions (I_3^-, AsF_6^-, etc.) is formed. Counteranions are generated by reduction of acceptors. In the case of donor doping (n-type doping), an ionic complex that consists of negatively charged polymer chains and countercations (Na^+, K^+, etc.) is formed. Countercations are generated by oxidation of donors. Electrical conductivity can be controlled by the dopant content. Charge carriers are formed by chemical doping.

A deep understanding of creation, transport, and decay processes of charge carriers is important for understanding the electronic properties of conjugated polymers at both intact and doped states. The carrier in a conjugated polymer is not an electron or a hole, but a quasiparticle with structural changes of the polymer backbone, because of the strong electron–lattice interaction of the polymer. Solitons [14], polarons [15–17], and bipolarons [16–18] have been proposed as charge carriers. They are collectively called elementary excitations or self-localized excitations. They can, in principle, move along a polymer chain with geometrical changes and hop a polymer chain to a neighboring chain.

Actual samples of conjugated polymers have more or less disordered structures and a distribution of conjugation lengths. Thus, spectroscopic studies of well-defined model compounds including radical ions, divalent ions, and electronically excited states, are useful for a better understanding of the optical properties of conducting polymers. An introduction to the carriers in conjugated polymers is given in Section 2. In Section 3, we describe the electronic absorption spectra of neutral and doped polymers.

2. CHARGE CARRIERS IN CONJUGATED POLYMERS

2.1. Ground-State Structures

The question of whether the C−C bonds in an infinite polyene chain are equal or alternate in length has been discussed by quantum chemists since the 1950s [19, 20]. Bond alternation is closely related to the electronic properties of the polymer. A structure that has bond alternation is expected to be a semiconductor, because of the existence of bandgap. On the other hand, a structure that has no bond alternation is expected to be a metal, because of the nonexistence of bandgap. Various experimental results on oligoenes have shown the existence of alternating single and double bonds. The bond alternation in *trans*-polyacetylene has been confirmed by X-ray [21] and nutation nuclear magnetic resonance (NMR) [22] studies. According to the nutation NMR study [22], the lengths of the C−C and C=C bonds in *trans*-polyacetylene are 1.44 and 1.36 Å, respectively. However, it is difficult to determine exact structure parameters for conducting polymers from X-ray diffraction studies, because single crystals of the polymers are unavailable. It is then useful to examine the structures of the polymers and model oligomers by molecular orbital (MO) methods, especially at *ab initio* Hartree–Fock levels or in higher approximations, and density functional methods.

The ground states of conjugated polymers can be divided into two types: degenerate and nondegenerate. The total energy curve of a degenerate system in the ground state is schematically shown as a function of a structural deformation coordinate, R, in Figure 3; that for a nondegenerate system is shown in Figure 4. The prototype of degenerate polymers is *trans*-polyacetylene, which has alternating C−C and C=C bonds. There are two stable structures (A and B in Fig. 3) with alternating C−C and C=C bonds, whereas the structure with equal C−C bond lengths (C in Fig. 3) is unstable. The two stable structures are identical with each other and have the same total energy; in other word, they are degenerate. The C−C and C=C bond lengths are calculated to be 1.373 and 1.423, respectively, by extrapolation from bond lengths of *trans*-oligoenes calculated at the MP2/6-31G* level [23]. On the other hand, a nondegenerate polymer has no two identical structures in the ground state, namely, the benzenoid and quinoid structures as shown in Figure 4. Most conjugated polymers belong to this class. Let us consider polythiophene as an example of nondegenerate polymers. An *ab initio* MO calculation at the Hartree–Fock level with the 6-31G* basis set for α-terthiophene has shown that the C−C, C=C, and C−S bond lengths of the central ring are 1.430, 1.351, and 1.739 Å, respectively, and the interring C−C bond length is 1.464 Å [24]. Thus, polythiophene has a benzenoid structure and has bond alternation. Suppose a structural change from a benzenoid to quinoid structures. The energy of the quinoid structure is higher than that of the benzenoid. Degeneracy is lifted in this geometry.

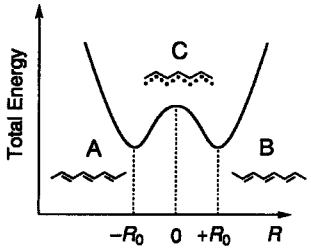

Fig. 3. Total energy as a function of a structural deformation coordinate R for *trans*-polyacetylene.

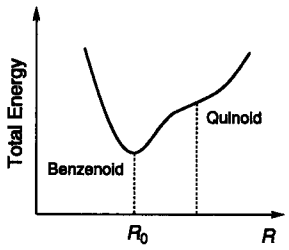

Fig. 4. Total energy as a function of a structural deformation coordinate R for a nondegenerate polymer.

2.2. Self-Localized Excitations

Types of self-localized excitations depend on the degeneracy of ground states. Consider polythiophene (Fig. 1c) as a typical nondegenerate polymer. The main process of chemical doping is the multistage oxidation (or reduction) reaction of conjugated polymer chains. In the case of acceptor doping, many electrons are removed from a polymer chain. The maximum charge transfer is typically about 7 mol% per carbon atom. When an electron is removed from an infinite polymer chain, charge +e and spin 1/2 are localized over several repeating units with structural changes (Fig. 5a). This is a self-localized excitation called a positive polaron. These structural changes associated with charge transfer are due to an electron–lattice (electron–phonon) interaction. For an oligomer, it is well known that the equilibrium geometry of a charged state is different from that of the neutral state. When another electron is removed from the positive polaron, charge +2e is localized over several rings (Fig. 5b). This species is called a positive bipolaron. A positive bipolaron has charge +2e and no spin. If a bipolaron is unstable, two polarons are formed as schematically shown in Figure 5c. Although the charge and spin are depicted as being localized on one carbon atom in Figure 5a–c, it has to be borne in mind that they extend over several rings with geometrical changes in real polymers. In the case of donor doping, a negative polaron and a negative bipolaron can be formed. Solitons are expected only for degenerate polymers such as *trans*-polyacetylene. Solitons can be formed between the A and B phases (Fig. 3). Solitons are classified into neutral, positive, and negative types according to their charges. A neutral soliton has no charge and spin 1/2. A positive (or negative) soliton has charge +e (or −e) and no spin. Solitons are nothing but bond-alternation defects or misfits in polyenes that were studied by the Hückel method in the early 1960s [19]. Self-localized excitations expected for conjugated polymers are listed in Table I. The self-localized excitations of conjugated polymers can be separately detected by electronic absorption, vibrational spectroscopy and electron-spin-resonance spectroscopy. In particular, electronic absorption spectroscopy gives us useful information on the electronic excitations in conjugated polymers.

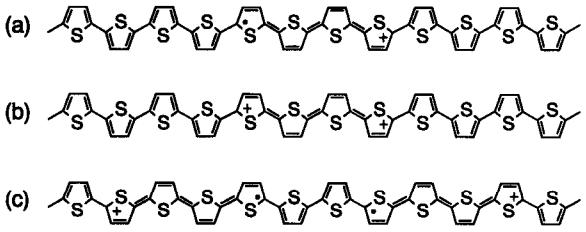

Fig. 5. Schematic structures of self-localized excitations in polythiophene: (a) a positive polaron, (b) a positive bipolaron, and (c) two positive polarons.

Table I. Self-localized Excitations and Chemical Terminologies

Self-localized excitation	Chemical term	Charge	Spin
Positive polaron	Radical cation	+e	1/2
Negative polaron	Radical anion	−e	1/2
Positive bipolaron	Closed-shell dication	+2e	0
Negative bipolaron	Closed-shell dianion	−2e	0
Neutral soliton	Neutral radical	0	1/2
Positive soliton	Cation	+e	0
Negative soliton	Anion	−e	0
Singlet exciton	S_1	0	0
Triplet exciton	T_1	0	1

3. ELECTRONIC SPECTRA

3.1. Neutral and Charged Oligomers

3.1.1. Oligothiophenes

The electronic absorption spectra of unsubstituted and substituted α-oligothiophenes have been reported [25–37]. Whereas the solubilities of unsubstituted oligothiophenes are low, various types of substituted oligothiophenes (Fig. 6) have been synthesized. As far as I know, the longest oligothiophene synthesized is a heptacosamer, which has 27 thiophene rings and shows absorption at 461 nm (2.69 eV) [34]. Neutral oligomers show an intense broad absorption band in the visible region. In most cases, vibrational progressions are not observed. The absorption band is assigned to the π-π^* transition. The absorption maxima and molar absorption coefficients are listed in Table II. The absorption maxima are plotted as closed triangles against the number of thiophene rings in Figure 7.

The radical cation and the divalent cation of each oligothiophene are model compounds of charge carriers in polythiophene. Thus, electronic absorption spectra of the radical cations and dications of oligothiophenes have been studied [26, 28–31, 33, 35, 38–46]. Oligothiophenes can be oxidized chemically by using oxidants such as $FeCl_3$ [38] and $THI^{\cdot+}(ClO_4^-)$ [35] (THI, thianthrene). For short-chain oligomers, a neutral oligomer is stepwise oxidized to its radical cation and dication. In the $FeCl_3$ oxidation processes, the reactions

$$T + 2FeCl_3 \rightarrow T^{\cdot+} + FeCl_4^- + FeCl_2$$

Table II. Absorption Maximum (λ_{max}) and Molar Absorption Coefficient (ε) for Oligothiophenes

Oligomer[a]	λ_{max} (nm) (eV^{-1})	ε ($mol^{-1}\,dm^3\,cm^{-1}$)	Solvent	Ref.
2T	302 (4.11)	12,500	Chloroform	[25]
3T	355 (3.49)	25,000	Chloroform	[25]
4T	390 (3.18)	45,500	Chloroform	[25]
5T	416 (2.98)	55,200	Chloroform	[25]
6T	432 (2.87)	60,000	Chloroform	[25]
2Dod-6T	425(2.92)	—	Dichloromethane	[35]
2Bu-7T	441 (2.81)	50,500	Dioxane	[37]
6Hex-9T	440 (2.82)	—	Chloroform	[32]
3Dod-9T	451 (2.75)	—	Dichloromethane	[35]
4Dec-12T	465 (2.67)	110,000	Chloroform	[29]
8Oct-13T	453 (2.74)	93,700	Tetrahydrofuran	[34]
10Hex-15T	456 (2.72)	—	Chloroform	[32]
12Oct-20T	461 (2.69)	151,700	Tetrahydrofuran	[34]
16Oct-27T	461 (2.69)	211,400	Tetrahydrofuran	[34]

[a] *m*R*n*T, α-oligothiophenes with *n* thiophene rings; *m*, the number of substituents; *R*, substituent; Dod, dodecyl; Bu, butyl; Hex, hexyl; Dec, decyl; Oct, octyl.

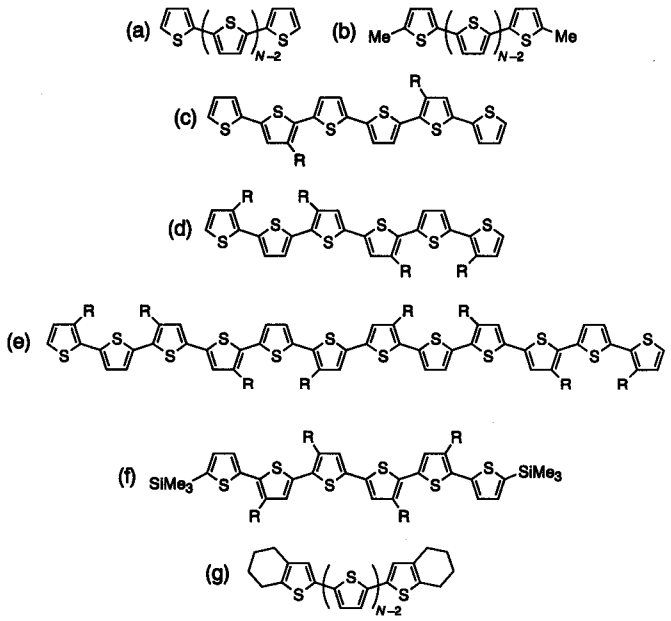

Fig. 6. Chemical structures of α-oligothiophenes: (a) unsubstituted oligothiophenes; (b) dimethyloligothiophenes (Me: CH_3); (c) and (d) partly β-substituted sexithiophenes (R: $C_{10}H_{21}$, $C_{12}H_{25}$); (e) partly β-substituted dodecamer (R: $C_{10}H_{21}$, $C_{12}H_{25}$); (f) partly β-substituted disilylsexithiophene (R: n-C_4H_9); (g) end-capped oligothiophenes.

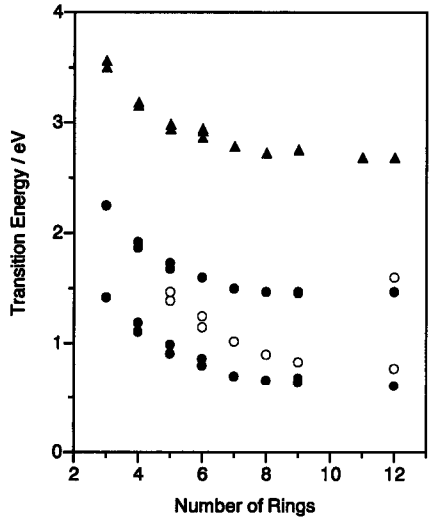

Fig. 7. Observed electronic transition energies of α-oligothiophenes in various states: ▲, neutral species; •, radical cation; o, dication.

$$T^{\cdot+} + 2FeCl_3 \rightarrow T^{2+} + FeCl_4^- + FeCl_2$$

occur, where T is an oligothiophene. In the oxidation with $THI^{\cdot+}(ClO_4^-)$, the reactions

$$T + THI^{\cdot+} \rightarrow T^{\cdot+} + THI$$
$$T^{\cdot+} + THI^{\cdot+} \rightarrow T^{2+} + THI$$

occur. In this case, the extent of oxidation can be measured by absorbance of the band due to the reduced THI. The radical cation gives rise to an electron-spin-resonance (ESR) signal, whereas the dication gives rise to no ESR signal.

The changes of the electronic absorption spectrum of a substituted sexithiophene (Fig. 6d; R = C_6H_{13}) upon the $THI^{\cdot+}(ClO_4^-)$ oxidation in a dichloromethane (CH_2Cl_2) solution are shown in Figure 8a [47]. The neutral oligomer gives rise to an absorption band at 3.00 eV. Two strong bands observed at 0.83 and 1.60 eV are attributed to the radical cation of the hexamer, whereas the intense band observed at 1.19 eV is attributed to the dication of the hexamer. Two peaks at 1.40 and 1.56 eV are attributable to vibrational transitions. The radical cation of each oligomer shows two intense bands.

A substituted dodecamer with 12 thiophene rings (Fig. 6e; R = C_6H_{13}) shows quite different spectral changes upon oxidation. The spectral changes of the dodecamer upon the $THI^{\cdot+}(ClO_4^-)$

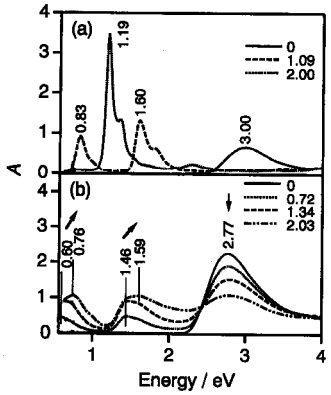

Fig. 8. Spectral changes of (a) β-substituted hexamer and (b) β-substituted dodecamer upon the $THI^{\cdot+}(ClO_4^-)$ oxidation in CH_2Cl_2 solution. The inset keys show the number of equivalents of $THI^{\cdot+}(ClO_4^-)$ added.

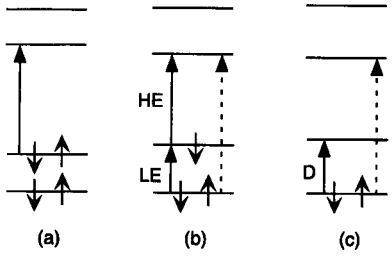

Fig. 9. Molecular orbital energy-level diagrams of (a) the neutral species, (b) the radical cation, and (c) the dication of an oligomer.

oxidation in dichloromethane are shown in Figure 8b. In these spectra, the stepwise oxidation reactions from neutral species to the radical cation and the dication are not observed, in contrast to the case of the hexamer. At low oxidation levels, two bands appear at 0.60 and 1.46 eV. Upon further oxidation, two bands at 0.76 and 1.59 eV become strong, whereas the 2.77-eV band attributed to neutral species is still observed. These spectral changes originate from the disproportionation reaction of the radical cation of the dodecamer [35]:

$$2(12T^{\cdot+}) \rightleftarrows 12T + 12T^{2+}.$$

The 0.60- and 1.46-eV bands are attributed to the radical cation of the dodecamer, whereas 0.76- and 1.59-eV bands are ascribed to the dication of the dodecamer. Similar spectral changes were reported by van Haare et al. [35] for a dodecamer with different alkyl substituents. They also clarified that the divalent cation is singlet by using ESR spectroscopy.

The observed transition energies of radical cations versus the number of thiophene rings are plotted in Figure 7 as solid circles. Each radical cation gives rise to two bands in the near-infrared region [low energy (LE) band] and in the visible region [high energy (HE) band]. As the number of thiophene rings increases, the transition energy associated with the LE or HE band converges to a finite value. The molecular orbital diagram of the radical cation of an oligothiophene is shown in Figure 9b; the neutral state and the dication of the oligomer are shown in Figure 9a and c, respectively. The LE and HE bands of the radical cation of each oligothiophene are indicated by arrows in Figure 8b [31, 44, 48–50]. These transitions are dipole allowed and polarized along the chain

Table III. Optical Transition Energies (in eV) of Radical Cation Monomers and Dimers of Oligothiophenes

Oligomer[a]	Monomer LE	Monomer HE	Dimer D_1	Dimer D_2	Dimer D_0	ΔH (kJ mol^{-1})	Ref.
2Me-3T	1.41	2.17	1.75	2.66	1.43	−42	[41]
EC-3T	1.32	2.00	1.63	2.57	1.25	—	[31]
EC-4T	1.05	1.79	1.37	2.25	1.09	−58	[31]
EC-5T	0.99	1.71	1.19	2.10	0.93	−65	[31]
EC-6T	0.84	1.59	0.98	1.81	—	—	[30]
2Dod-6T	0.87	1.60	1.12	1.81	—	−88	[30]
3Dod-9T	0.67	1.46	0.95	1.94	—	−61	[35]

[a] 2Me-3T, dimethylterthiophene (see Fig. 6b); EC-*n*T, end-capped oligothiophenes (see Fig. 6g); other abbreviations, see the footnote to Table II.

axis [44, 48]. For the charged oligomers with C_{2h} symmetry, the transition shown as a dotted arrow is dipole forbidden [44, 49, 50]. For the charged oligomers with C_{2v} symmetry, this transition is extremely weak, because the transition is polarized in the direction perpendicular to the chain axis [44, 48].

There are three possible states for the dication of an oligothiophene: closed-shell (bipolaronic structure), singlet biradical (two-polaron structure), and triplet biradical (two-polaron structure) [35, 51, 52]. The observed transition energies of dications versus the number of thiophene rings are plotted in Figure 7 as open circles. The dications of oligothiophenes up to nonamer give rise to one strong band (D band) and have closed-shell structures. The molecular orbital diagram of the closed-shell dication is shown in Figure 9c. The D band of the dication of each oligothiophene is indicated by an arrow in Figure 9c [46, 49]. This transition is dipole allowed and polarized along the molecular chain axis [31, 44, 48–50]. For the charged oligomers with C_{2h} symmetry, the transitions indicated by dotted arrows are dipole forbidden [44, 49, 50]. For the charged oligomers with C_{2v} symmetry, this transition is extremely weak, because the transition is polarized in the direction perpendicular to the molecular chain axis [44, 48]. The transition energy associated with the D band due to the dications decreases more rapidly than the energy associated with the LE and HE bands (see Fig. 7). It is surprising that the dication of dodecamer gives rise to two band, whereas the dications of oligothiophenes up to nonamer give rise to one intense band. This result probably indicates that the bipolaronic charged domain on a dication continues to expand with increasing number of rings. Then, the dication of duodecithiophene takes the singlet biradical state (two-polaron structure).

Hill et al. [40, 41] and Bäuerle et al. [30, 31] reported the singlet π-dimer formation of the radical cations of oligothiophenes. Upon lowering the temperature of a solution of a radical cation, the LE and HE bands of the radical cation show blue shifts, and an ESR signal that originates from the radical cation disappears. Consequently, the new absorption bands have been ascribed to the singlet π-dimer of the radical cations. These absorption bands due to the dimer are called D_1 and D_2 herein. A band that appears in the near-infrared range upon dimer formation is called D_0. The observed positions of the D_0, D_1, and D_2 bands are listed in Table III. There exists a monomer–dimer equilibrium,

$$2T^{\cdot+} \rightleftarrows (T_2)^{2+}$$

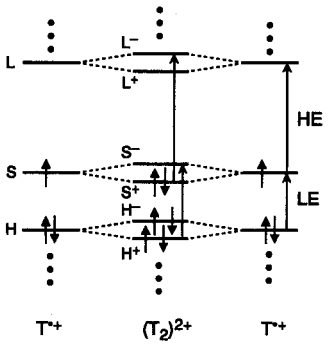

Fig. 10. Molecular orbital energy-level diagram for a singlet dimer of the radical cation of an oligothiophene.

where T is an oligothiophene. The enthalpies of dimer formation were obtained by van't Hoff plots for electronic absorption or ESR measurements, and they are listed in Table III. Bäuerle et al. [31] proposed the tentative assignments of the D_0, D_1, and D_2 bands within the framework of the Hückel theory. They also proposed the energy-level diagram of a radical–cation dimer (Fig. 10). A molecular orbital of the dimer is constructed by the linear combination of the orbitals of the monomers; each monomer level (such as L, S, and H in Fig. 10) is thus split into energetically lower (such as L^+, S^+, and H^+) and higher levels (such as L^-, S^-, and H^-). As a result, the levels of the dimer are fully occupied or unoccupied. This is in agreement with the experimental result that the ESR signal of the radical–cation monomer disappears upon dimer formation. Let us assume that the dimer has inversion symmetry. The D_1 band has been attributed to the transition between the H^+ and S^- levels, and the D_2 band is attributed to the transition between the S^+ and L^- levels [31]. In the case of unsubstituted and partly β-substituted hexamers, radical–cation dimers are present at room temperature [30]. On the other hand, no bands due to radical–cation dimers have been observed at room temperature for partly β-substituted disilyloligothiophenes [28].

The photoexcitations of oligothiophenes were reviewed by Janssen [53]. Fluorescence is observed for oligothiophenes. The observed fluorescence band has been assigned to the dipole-allowed transition from the S_1 state that is derived from the ground state by the promotion of one electron from the highest occupied molecular level (HOMO) to the lowest unoccupied molecular level (LUMO) [54–57]. The maximum wavelengths and quantum efficiencies of oligothiophenes [37] are listed in Table IV. The electronic absorption spectra of the S_1 states were measured in the range from 1.3 to 2.9 eV by the Kerr ellipsometry method [58] and pump-probe time-resolved spectroscopy [59, 60]. One strong photoinduced band was obtained for each oligothiophene; this band was attributed to the $S_n \leftarrow S_1$ transition. Electronic absorption spectra attributed to the $T_n \leftarrow T_1$ transition of oligothiophenes have been reported [60–62]. The transition energy of each oligothiophene shows a downshift in going from a solution to a solid film; for example, the T_1 state of an undecamer gives rise to the band at 1.54 eV in a CH_2Cl_2 solution and at 1.26 eV in a solid film [62]. With increasing number of thiophene rings, the $T_n \leftarrow T_1$ and $S_n \leftarrow S_1$ transition energies decrease. The position of the $T_n \leftarrow T_1$ transition is higher than that of the $S_n \leftarrow S_1$ transition for each oligothiophene. The molecular and electronic structures of oligothiophenes have been calculated by using semiempirical molecular orbital methods [63–65].

Table IV. Maximum Wavelength (λ_F) and Quantum Efficiency (ϕ_F) of Fluorescence at Room Temperature for Oligothiophenes

Oligomer[a]	λ_F (nm) (eV^{-1})	ϕ_F	Solvent/matrix	Ref.
2T	362 (3.42)	0.017	Dioxane	[37]
3T	407 (3.05)	0.066	Dioxane	[37]
4T	437 (2.84)	0.18	Dioxane	[37]
5T	482 (2.57)	0.36	Dioxane	[37]
6T	502 (2.47)	0.41	Dioxane	[37]
2Bu-7T	522 (2.38)	0.34	Dioxane	[37]
8Oct-13T	554 (2.24)	—	Tetrahydrofuran	[34]
12Oct-20T	559 (2.22)	—	Tetrahydrofuran	[34]
16Oct-27T	560 (2.21)	—	Tetrahydrofuran	[34]

[a]Abbreviations as cited in the footnote to Table II.

Table V. Absorption Maximum (λ_{max}) and Molar Absorption Coefficient (ε) for *p*-Oligophenyls in Chloroform[a]

Number of rings	λ_{max} (nm) (eV^{-1})	ε ($mol^{-1}\,dm^3\,cm^{-1}$)
2	251.5 (4.93)	18,300
3	280 (4.43)	25,000
4	300 (4.13)	39,000
5	310 (4.00)	62,500
6	317.5 (3.90)	>56,000

[a]Data from [66].

3.1.2. *Oligophenyls*

The electronic absorption spectra of unsubstituted and substituted *p*-oligophenyls have been reported [66–68]. Each oligomer shows an intense absorption in the ultraviolet region. The band is assigned to the π-π^* transition. The absorption maxima of biphenyl, *p*-terphenyl, *p*-quaterphenyl, *p*-quinquephenyl, and *p*-sexiphenyl are listed in Table V. The electronic absorption spectra of *p*-oligophenyls in the radical–anion and dianion states have been studied [68–75]. Furukawa et al. [73] showed that neutral terphenyl is stepwise reduced to its radical anion and dianion in tetahydrofuran by using sodium (Na). In these reduction processes, the reactions

$$P + Na \rightarrow P^{\cdot -} + Na^+$$
$$P^{\cdot -} + Na \rightarrow P^{2-} + Na^+$$

occur, where P is an oligophenyl. The reported transition energies [72–74] of the radical anions and the dianions in solutions are listed in Table VI. Each radical anion gives rise to two strong absorption bands: the LE and HE. On the other hand, each dianion gives rise to one strong band; this band is called D. The transition energies associated with the LE, HE, and D bands decrease with increasing number of rings. The transition energies due to the dianions (D band) decrease more rapidly than those due to the radical anions (LE and HE bands). This is also observed for the dications of oligothiophenes described previously. Buschow et al. [69] reported that the positions of the absorption bands due to the radical anions depend on the nature of solvents and counteri-

Table VI. Absorption Maxima of the Radical Anions and the Dianions of *p*-Oligophenyls in Solutions

	Radical anion				
Number of rings	LE (nm) (eV^{-1})	HE (nm) (eV^{-1})	Ref.	Dianion	Ref.
2	637 (1.95)	405 (3.06)	[69]	—	—
3	916 (1.35)	481 (2.58)	[73]	650 (1.91)	[73]
4	1205 (1.03)	518 (2.39)	[73]	775 (1.60)	[73]
5	1390 (0.89)	544 (2.28)	[73]	997 (1.24)	[73]
6	1560 (0.79)	558 (2.22)	[73]	1170 (1.06)	[73]

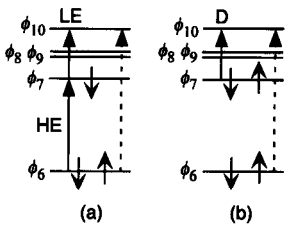

Fig. 11. Molecular orbital energy-level diagrams of (a) the radical anion and (b) the dianion of biphenyl.

ons; they discussed these observations in light of free ions and ion pairs.

Zahradník and Cársky [75] studied the electronic absorption spectrum of the radical anion of biphenyl using the Pariser–Parr–Pople method combined with a limited configuration interaction (CI). The molecular orbital energy-level diagram of the radical anion is similar to that shown in Figure 11. The ϕ_8 and ϕ_9 orbitals are associated with the transitions that have dipole moments perpendicular to the molecular long axis and very weak intensity. The LE and HE bands primarily originate from the transitions shown in Figure 11. Rubio et al. [76] calculated the electronic transition energies associated with the radical anion and radical cation of biphenyl using an *ab initio* multiconfigurational second-order perturbation theory (CASPT2). They interpreted the transition energies quantitatively and demonstrated the configurational nature of the transitions. It is reasonable to consider that the LE and HE bands of the radical anions of oligophenyls have natures similar to those of the LE and HE bands of the radical anion of biphenyl, respectively [73]. Note that the transitions indicated by dotted arrows are dipole forbidden under the planar structure with D_{2h} symmetry [73].

3.1.3. *Oligophenylenevinylenes*

Electronic absorption spectra of unsubstituted and substituted oligo-*p*-phenylenevinylenes (Fig. 12) in the neutral, radical–anion, dianion, and radical–cation states have been reported [77–87]. Neutral oligomers show an intense visible absorption band attributed to the π-π^* transition. The absorption wavelengths and molar absorption coefficients are tabulated in Table VII. Because the charged species are easily decomposed in the presence of a small amount of oxygen or water, contradictory experimental results were reported for the charged species of these oligomers. The data that seem to be most reliable have been selected from the reported articles. The transition energies of the radical anions and dianions are listed in Table VIII [88]; those of the radical

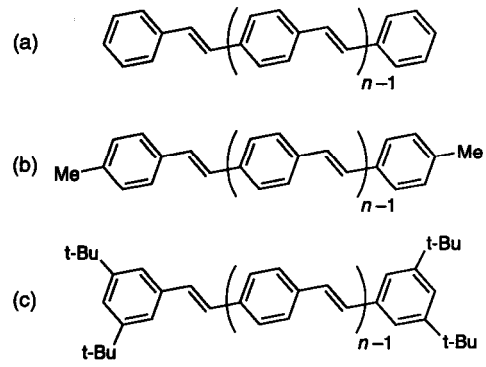

Fig. 12. Chemical structures of oligo-*p*-phenylenevinylenes. Me, CH_3; t-Bu, $C(CH_3)_3$.

cations are listed in Table IX. Each radical anion gives rise to two strong absorption bands (called LE and HE), and so does each radical cation. Each dianion gives rise to one strong absorption band (called D). The transition energy due to the D band of the dianions decreases more rapidly than those due to the LE and HE bands of the radical anions. Note that the formation of dianions has not been reported for long oligomers (the number of vinylene groups $N = 5$ and 6). The observed transition energies of the LE and HE bands are quite similar to those of the radical cation for each oligomer.

Karabunarliev et al. [89] studied the electronic absorptions associated with the radical anions of oligophenylenevinylenes using the Pariser–Parr–Pople/CI method on the basis of the structures obtained from the AM1 method. Cornil et al. [90] studied the radical anions and dianions of oligophenylenevinylenes by means of the intermediate neglect of differential overlap (INDO) CI method on the basis of the structures obtained from the AM1 method. According to their calculations, the LE and HE bands of each radical anion are assigned to the transitions indicated by arrows in Figure 13b, because the CI expansion coefficients of the corresponding configurations are predominant. On the other hand, the D band of each dianion is attributed to the transition indicated by an arrow in Figure 13c [90].

The radical–cation dimer of the oligophenylenevinylene ($n = 2$) is formed at low temperatures [91]. The radical cation gives rise to two bands at 1.03 and 1.95 eV, whereas the dimer gives rise to two bands at 1.26 and 2.36 eV. The observed blue shifts are 0.23 and 0.41 eV for the LE and HE bands, respectively. The enthalpy of dimer formation is 53 kJ mol^{-1}. These blue shifts and the enthalpy of formation are similar to those reported for the radical–cation dimers of oligothiophenes (see Table III).

Strong fluorescence is observed for oligophenylenevinylenes [77, 86]. The observed wavelengths are tabulated in Table X. The T_1 state of *trans*-stilbene was observed by means of flash photolysis [92]. The electronic absorption spectra associated with the triplet states of oligophenylenevinylenes (n = 2–6) in KBr pellets were measured in the range from 1.3 to 2.3 eV [86]. Each oligomer gives rise to one strong absorption band attributed to the $T_n \leftarrow T_1$ transition [93–95]. For examples, 4Bu-PV2 gives rise to the band at 2.12 eV and 4Bu-PV6 gives rise to the band at 1.61 eV. Among oligophenylenevinylenes, the $S_n \leftarrow S_1$ absorption band of *trans*-stilbene was observed at 2.12 eV in a hexane solution [96]. The chain-length dependence of the $S_n \leftarrow S_1$ transitions has not been clarified yet.

Table VII. Absorption Maxima (λ_{max}) and Molar Absorption Coefficients (ε) of Oligo-*p*-phenylenevinylenes

Oligomer[a]	λ_{max} (nm) (eV^{-1})	ε ($mol^{-1}\ dm^3\ cm^{-1}$)	Solvent	Ref.
PV1	295 (4.20)	—	Hexane	[77]
2Me-PV1	317 (3.91)	—	Tetrahydrofuran	[85]
PV2	350 (3.55)	—	Hexane	[77]
2Me-PV2	360 (3.44)	—	Tetrahydrofuran	[85]
4Bu-PV2	359.8 (3.45)	56,200	Chloroform	[82]
PV3	385 (3.22)	—	Chloroform	[77]
2Me-PV3	386 (3.21)		Tetrahydrofuran	[85]
4Bu-PV3	386.9 (3.20)	87,100	Chloroform	[82]
PV4	385 (3.22)	—	Dioxane	[77]
4Bu-PV4	402.7 (3.08)	112,000	Chloroform	[82]
PV5	388 (3.20)	—	Dioxane	[77]
4Bu-PV5	412 (3.01)	112,000	Chloroform	[82]
PV6	388 (3.20)	—	Dioxane	[77]
4Bu-PV6	417.9 (2.97)	135,000	Chloroform	[82]
4Bu-PV7	415 (2.99)	—	Chloroform	[82]

[a] *m*R-PV*n*: *m*, the number of substituents; R, substituents; Me, methyl; Bu, butyl; *n*, the number of vinylene groups. PV*n*, see Fig. 12a; 2Me-PV*n*, see Fig. 12b; 4Bu-PV*n*, see Fig. 12c.

Table VIII. Absorption Maxima of the Radical Anions and the Dianions of Oligo-*p*-phenylenevinylenes in Solutions

	Radical anion				
Oligomers[a]	LE (nm) (eV^{-1})	HE (nm) (eV^{-1})	Ref.	Dianion	Ref.
2Me-PV1	694 (1.79)	488 (2.54)	[85, 88]	520 (2.38)	[85]
4Bu-PV1	699 (1.77)	492 (2.52)	[81]	504 (2.46)	[81]
2Me-PV2	1136 (1.09)	631 (1.96)	[85, 88]	794 (1.56)	[85]
4Bu-PV2	1085 (1.14)	612 (2.03)	[81]	805 (1.54)	[81]
2Me-PV3	1449 (0.86)	711 (1.74)	[85, 88]	965 (1.28)	[85]
4Bu-PV3	1453 (0.85)	712 (1.74)	[81]	979 (1.27)	[81]
4Bu-PV4	1720 (0.72)	759 (1.63)	[81]	1176 (1.05)	[81]
4Bu-PV5	1923 (0.64)	786 (1.58)	[81]	—	—
4Bu-PV6	1976 (0.63)	794 (1.56)	[81]	—	—

[a] Abbreviations as cited in the footnote to Table VII.

Table IX. Absorption Maxima of the Radical Cations and the Dication of Oligo-*p*-phenylenevinylenes in Solutions[a]

	Radical cation		
Oligomer[b]	LE (nm) (eV^{-1})	HE (nm) (eV^{-1})	Dication
2Me-PV1	804 (1.54)	507 (2.45)	—
2Me-PV2	1200 (1.03)	636 (1.95)	990 (1.25)
2Me-PV3	1550 (0.80)	713 (1.74)	—

[a] Data from [87].

[b] See Figure 12b.

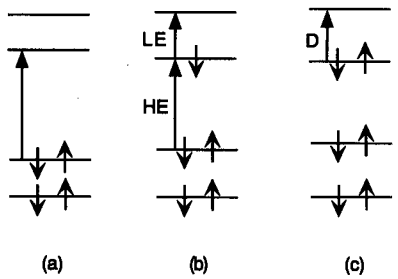

Fig. 13. Molecular orbital energy-level diagrams of (a) the neutral species, (b) the radical anion, and (c) the dianion of a oligomer.

3.1.4. Oligoenes

The electronic spectra of oligoenes (which are also called polyenes) have been reviewed elsewhere [20, 97–99]. Whereas unsubstituted oligoenes are not stable, various types of substituted oligoenes have been studied. The absorption bands or peaks of all-trans conformers of unsubstituted oligoenes (Fig. 14a) [100–102], α,ω-dimethyloligoenes [101, 103, 104], α,ω-di-*tert*-butyloligoenes

Table X. Fluorescence Maximum Wavelengths of Oligo-*p*-phenylenevinylenes in KBr[a]

Oligomer[b]	λ_F (nm) (eV^{-1})
PV1	362 (3.42)
PV2	444 (2.79)
PV3	493 (2.52)
PV4	521 (2.38)
PV5	521 (2.38)

[a]Data from [77].

[b]See Figure 12a.

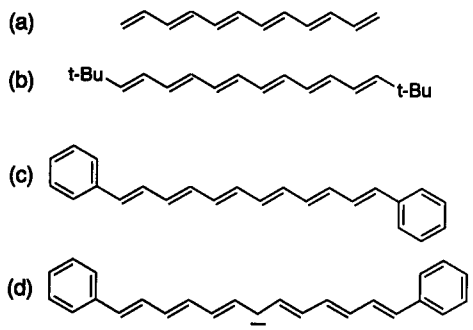

Fig. 14. Schematic chemical structures of *trans*-oligoenes at neutral and charged states: (a) unsubstituted oligoenes; (b) α,ω-dibutyloligoene; (c) α,ω-diphenyloligoene (N_C = 12); (d) α,ω-diphenyloligoenyl anion (N_C = 13).

Table XI. Absorption Maximum (λ_{max}) of All-*trans*-α,ω-di-tert-butylpolyenes in *n*-Pentane[a]

$N_{C=C}$	λ_{max} (nm) (eV^{-1})
2	237.2 (5.23)
3	275.6 (4.50)
4	311.4 (3.98)
5	343.0 (3.61)
6	371.2 (3.34)
7	396.2 (3.13)
8	418.8 (2.96)
9	438.8 (2.83)
10	456.4 (2.72)
11	468.8 (2.64)
13	494 (2.51)

[a]Data from [105].

(Fig. 14b) [105], α,ω-diphenyloligoenes (Fig. 14c) [106, 107], and α,ω-dithienyloligoenes [108] have been reported. Each oligoene gives rise to an intense absorption with several peaks attributed to vibrational transitions in the ultraviolet or visible region. Note that the positions of electronic absorption bands strongly depend on solvents [20, 98]. This absorption band is dipole allowed, because the molar absorption coefficient is very large. Although the observed absorption peaks are due to vibrational transitions, a

Table XII. Absorption Maximum (λ_{max}) of All-*trans*-α,ω-diphenylpolyenes in Benzene[a]

$N_{C=C}$	λ_{max} (nm) (eV^{-1})
1	319 (3.89)
2	352 (3.52)
3	377 (3.29)
4	404 (3.07)
5	424 (2.92)
6	445 (2.79)
7	465 (2.67)

[a]Data from [107].

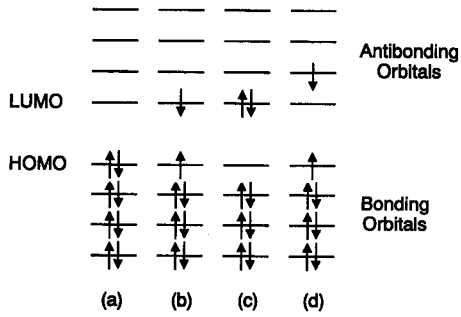

Fig. 15. Some configurations that describe the low energy singlet states of an oligoene.

precise vibrational analysis cannot be made because of the broad bandwidths. The position of the longest maximum in absorption spectra for α,ω-di-*tert*-butylpolyenes and α,ω-diphenylpolyenes are listed in Tables XI and XII, respectively. Although these absorption maxima (λ_{max}) depend on the kind of substituents, they increase with increasing number of C=C bonds ($N_{C=C}$).

Let us consider an unsubstituted linear oligoene with N C=C double bonds, that is, $2N$ π-electrons. The number of molecular orbitals equals the number of π-electrons. These molecular orbitals can be classified into two types: N bonding and N antibonding. The three low-lying singlet states of linear oligoenes are described [20, 98] in terms of the configurations shown in Figure 15. The ground state S_0 is well described by the single configuration in which the N bonding orbitals are doubly occupied (Fig. 15a). The second excited state S_2 is described by the single configuration that is derived from the ground state by promoting one electron from the HOMO to the LUMO, as shown in Figure 15b. On the other hand, the S_1 state is a correlated state that cannot be written in terms of a single configuration because of electron correlation, but is approximately described by a linear combination of the doubly excited configuration in which two electrons are promoted from the HOMO to the LUMO (Fig. 15c) and the double jump configuration in which one electron is promoted from the HOMO to the LUMO+1 (Fig. 15d). Electron correlation is essential for a correct description of the electronic state ordering for linear oligoenes. (In most conjugated oligomers except for linear oligoenes, the ordering of S_1 and S_2 is reversed.) In the all-trans planar structure (C_{2h} symmetry), S_0 and S_1 have A_g symmetry and are called $1\,^1A_g$ and $2\,^1A_g$, respectively; S_2 has B_u symmetry and is called $1\,^1B_u$. As a result, the transition between S_0 and S_1 is dipole forbidden,

whereas the transition between S_0 and S_2 is dipole allowed. The intense absorptions described in the foregoing text are attributed to the $1\,^1B_u \leftarrow 1\,^1A_g$ transitions (π-π^* transitions). This is a general property of linear oligoenes of all chain lengths independent of local symmetry and/or the presence of cis bonds. This is why the labels $1\,^1A_g$ for S_0, $2\,^1A_g$ for S_1, and $1\,^1B_u$ for S_2 are used in the literature on oligoenes even in cases where C_{2h} symmetry is not realized. Ordering that locates the $2\,^1A_g$ excited state below the $1\,^1B_u$ excited state is peculiar to linear oligoenes. The ordering of the A_g and B_u excited states is associated with fluorescence for conjugated oligomers.

The observed $1\,^1B_u \leftarrow 1\,^1A_g$ (0–0) transition energy, E_n, has been expressed as a function of the number of C=C double bonds ($N_{C=C}$) fitted by the equation [105]

$$E_n(\text{eV}) = E_\infty + \frac{k}{N_{C=C}} \quad (1)$$

where E_∞ and k are constants. From observed transition energies of α,ω-dibutyloligoenes, E_∞ and k are determined to be about 1.56 and 9.5 eV, respectively, in carbon disulfide and about 1.79 and 9.4 eV in pentane [105]. The differences between these estimated values come from the fact that the observed transition energies are sensitive to solvents. Equation (1) suggests that the $1\,^1B_u$ transition energy goes to a finite limit (E_∞) at infinite chain length.

The position of the observed weak fluorescence for each oligoene shows a considerable red shift in comparison with the position of its absorption band. In other words, a large Stokes shift is observed. This emission band is due to the transition from the $2\,^1A_g$ excited state to the $1\,^1A_g$ ground state. The absorption band associated with the $2\,^1A_g \leftarrow {}^1A_g$ transition is not observed, because it is expected to be extremely weak. The transition energy for the $2\,^1A_g$ excited state is always lower than that for the $1\,^1B_u$ state for each polyene.

α,ω-Diphenyloligoenyl anions are model compounds of a negative soliton in *trans*-polyacetylene. The chemical structure of a diphenyloligoenyl anion is schematically shown in Figure 14d. These compounds with odd numbers of carbon atoms at the oligoene parts have a negative charge, but no spin. The radical anions of α,ω-diphenyloligoenes are model compounds of a negative polaron in *trans*-polyacetylene. These compounds with even numbers of carbon atoms at the oligoene parts have a negative charge and spin 1/2. The observed electronic transition energies [109–111] of these charged compounds are plotted versus the numbers of oligoene carbon atoms (N_C) in Figure 16. The radical anion of each diphenyloligoene gives rise to two absorption bands [109]. The transition energies associated with the radical anions are shown as solid circles in Figure 16. The LE band is weak in intensity and the HE band is strong [109]; these spectral features are quite different from those reported for the radical ions of the oligothiophenes, oligophenyls, and oligophenylenevinylenes. The LE and HE bands are attributed to the transitions indicated by arrows in Figure 12b, which are from the calculations performed by means of the Pariser–Parr–Pople and Longuet–Higgins and Pople methods, including all singly excited configuration interactions [112]. On the other hand, each diphenyloligoenyl anion gives rise to one strong absorption band [100, 101], which is called band S. The transition energies of the S band are shown as open circles in Figure 16. The S band is ascribed to the transition from the nonbonding orbital to the LUMO shown in Figure 17 [112, 113]. Figure 16 shows that

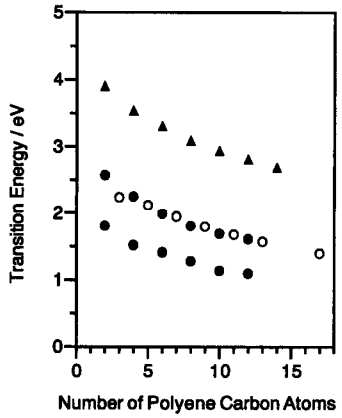

Fig. 16. Observed electronic transition energies of *trans*-oligoenes in various states. (a), ▲, neutral α,ω-diphenyloligoene; •, radical anion of α,ω-diphenyloligoenes; ○, α,ω-diphenyloligoenyl anion.

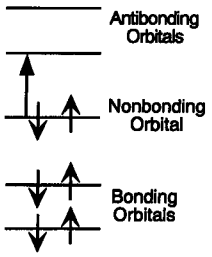

Fig. 17. Molecular orbital energy-level diagram of the anion of an odd oligoene.

Table XIII. Absorption Maxima of the Radical Cations of α,ω-Di-tert-butylpolyenes in Freon Matrix[a]

$N_{C=C}$	LE (nm) (eV^{-1})	HE (nm) (eV^{-1})
3	626 (1.98)	430 (2.88)
4	738 (1.68)	498 (2.49)
5	861 (1.44)	571 (2.17)
6	1000 (1.24)	653 (1.90)
7	1180 (1.05)	734 (1.69)
8	1270 (0.98)	800 (1.55)
9	1440 (0.86)	879 (1.41)
11	1720 (0.72)	1010 (1.23)
13	1970 (0.63)	1110 (1.12)

[a]Data from [114].

the transition energies associated with the HE band are coincident with those associated with the S band. Parkes and Young [110] reported that the positions of the S band in diphenyloligoenyl anions strongly depend on the nature of solvents; these properties have been explained by the presence of loose ion pairs and tight ion pairs [110].

The radical cations of polyenes are models of a positive polaron in *trans*-polyacetylene. The electronic absorption spectra of the radical cations of α,ω-dibutyloligoenes have been reported [114]. The observed absorption maxima of the radical cations [114] of dibutyloligoenes are listed in Table XIII. Each radical cation gives

rise to two absorption bands: the LE band is weak in intensity and the HE band is strong. These spectral features are similar to those of the radical anions of diphenyloligoenes. According to studies performed by molecular orbital methods [114, 115], the intensities of the LE and HE bands have been explained by the configuration interactions.

The T_1 states of oligoenes including carotenoids have been studied by means of flash photolysis [116, 117]. Each oligoene gives rise to one strong absorption band attributed to the $T_n \leftarrow T_1$ transition. Note that spectra in the range below 1.88 eV have not been reported. The observed energies decrease with increasing $N_{C=C}$.

3.2. Neutral and Doped Polymers

The absorption of conjugated polymers appears in the region from ultraviolet to near-infrared. The optical absorption spectra of conjugated polymers have been studied from the experimental and theoretical standpoints [2]. The excitonic effect is essential and significant in conjugated polymers, although the band picture is very useful for a rough understanding of the electronic properties of conjugated polymers. The discussions about exciton and band pictures have been reviewed previously [118]. The peak and band shape of absorption depend on the molecular weight, substituents, state, and defect content of the polymer. The observed maxima of absorption in some typical polymers are listed in Table XIV [119–125]. The band edges are usually 0.3–0.5 eV lower than these maxima. Thus, optical bandgaps of conjugated polymers are in the range from 1 to 3.5 eV.

The charge carriers in conjugated polymers are polarons, bipolarons, and charged solitons. The importance of spinless charge carriers, charged solitons, and bipolarons has been pointed out [119, 122, 126]. The charge carriers in conjugated polymers can be generated by chemical doping, electrochemical doping, or photoirradiation. The maxima of the subgap absorption due to charged excitations generated by chemical doping and photoirradiation are compiled in Table XV [88, 119, 122, 124, 127–133]. Table XV shows that there are one or two subgap absorption bands. The two-band features observed for nondegenerate polymers, such as polythiophene, poly(*p*-phenylene), polypyrrole, poly(*p*-phenylenevinylene), and poly(2,5-thienylenevinylene), were discussed previously with regard to spinless bipolarons. However, recent studies on charged model compounds have revealed that the two-band features can be attributed to polarons and the one-band feature to bipolarons [50, 134–138]. Excitons as well as carriers play an important role in optical properties of conjugated polymers. The photoexcitation dynamics associated with excitons and carriers have been studied on a time scale from femtosecond to millisecond [139, 140]. The major species on the micro- to millisecond time scale are carriers that are charged self-localized excitations and triplet excitons that are neutral excitations.

3.2.1. *Subgap Absorptions*

Theoretical consideration provided the basis for the assignments of doping- and photoinduced electronic absorptions in conjugated polymers. Energy-level diagrams of electronic excitations in conjugated polymers are shown in Figure 18, according to a continuum electron–phonon-coupled model proposed by Fesser, Bishop, and Campbell [141]. Note that the Fesser–Bishop–Campbell model is a continuum version of the Su–Schrieffer–Heeger model, which

Table XIV. Maximum of Absorption in Conjugated Polymer Films

Polymer	Maximum (eV)	State/solvent	Ref.
trans-Polyacetylene	1.9	Film	[122]
Polythiophene	2.6	Film	[122]
Poly(*p*-phenylene)	3.4	Film	[120]
Polypyrrole	3.2	Film	[119]
Poly(isothianaphthene)	1.4	Film	[122]
Poly(*p*-phenylenevinylene)	2.85	Film	[125]
Poly(2,5-thienylenevinylene)	2.3	Film	[121]
Polyaniline			
Leucoemeraldine base	3.8	Film	[123]
Emeraldine base	2.0, 3.8	*N*-methylpyrrolidinone	[124]
Pernigraniline base	2.3, 3.8	*N*-methylpyrrolidinone	[124]

Table XV. Maximum of Subgap Absorptions Due to Charged Excitations in the Film State

Polymer	Method	Maximum (eV)	Ref.
trans-Polyacetylene	AsF_6^- doping	0.7	[122]
	Na^+ doping	0.7	[122]
	Photodoping	0.48	[127]
Polythiophene	ClO_4^- doping	0.65, 1.5	[122]
	$N(n\text{-}Bu)_4^+$ doping	0.65, 1.65	[128]
	Photodoping	0.4, 1.3	[129]
	Photodoping	0.9	[129]
Poly(*p*-phenylene)	AsF_6^- doping	0.9, 2.1	[130]
	$N(n\text{-}Bu)_4^+$ doping	0.7, 2.4	[130]
Polypyrrole	ClO_4^- doping	1.0, 2.7	[119]
Poly(*p*-phenylenevinylene)	ClO_4^- doping	0.9, 2.3	[131]
	Na^+ doping	1.55	[88]
	Photodoping	0.6, 1.6	[132]
Poly(2,5-thienylenevinylene)	Photodoping	0.44, 1	[133]
Polyaniline			
Emeraldine salt	HCl treatment	1.4, 3.0	[124]

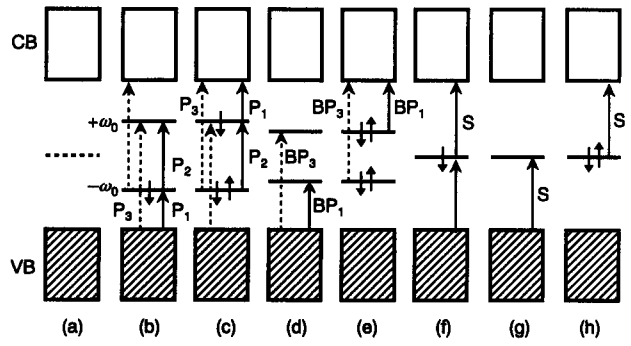

Fig. 18. Schematic electronic structures: (a) neutral polymer; (b) positive polaron; (c) negative polaron; (d) positive bipolaron; (e) negative bipolaron; (f) neutral soliton; (g) positive soliton; (h) negative soliton. CB, conduction band; VB, valence band. The full and dashed arrows represent allowed and forbidden optical transitions, respectively.

is a solid-state-physics version of the Hückel theory. The electronic transitions due to the electronic excitations can be correlated to those of the charged and electronically excited states of oligomers. In an infinite polymer chain, the interaction between repeating units leads to the formation of the valence band and the conduction band as shown in Figure 18a. The bandgap between the valence and conduction bands is expressed as $2\Delta_0$. For a polaron or a bipolaron, two localized electronic levels—bonding and antibonding—are formed symmetrically with respect to the gap center at $-\omega_0$ and $+\omega_0$, respectively (Fig. 18b–e), because of electron–hole symmetry. The positions of the localized electronic levels (i.e., $\pm\omega_0$) depend on the extent of the structural changes associated with the polarons and bipolarons. On the other hand, for solitons, one localized electronic level, which is nonbonding, is formed at the gap center (Fig. 18f and g).

3.2.1.1. *Polarons*

When a positive polaron is formed, one electron is removed from the $-\omega_0$ level (Fig. 18b). Thus, a positive polaron is expected to have the following intragap transitions:

- P_1 transition: $-\omega_0$ level ← valence band
- P_2 transition: $+\omega_0$ level ← $-\omega_0$ level
- P_3 transition: $+\omega_0$ level ← valence band, and conduction band ← $-\omega_0$ level

When a negative polaron is formed, one electron is added to the $+\omega_0$ level (Fig. 18c). In this case, three transitions are also expected. Within the Fesser–Bishop–Campbell model, the subgap absorptions due to the P_1 and P_2 transitions are much stronger than that due to the P_3 transition, because the P_3 transition is symmetry forbidden. Quantitatively, the intensities of these subgap absorptions are given as a function of the ratio ω_0/Δ_0.

The radical cations of oligothiophenes and oligophenylenevinylenes, and the radical anions of oligophenyls and oligophenylenevinylenes give rise to two strong absorption bands, as described in the previous sections. These observations indicate that two subgap absorptions are expected for a polaron in a nondegenerate polymer. The radical anions and radical cations of oligoenes give rise to one strong absorption band and one weak band, as described previously. These observations indicate that one strong subgap absorption and one weak subgap absorption are expected for a polaron in *trans*-polyacetylene. This is probably because electron–electron interactions, which are not taken into account in the Fesser–Bishop–Campbell model, have a strong effect on the optical absorptions of a polaron in *trans*-polyacetylene.

3.2.1.2. *Bipolarons*

When a positive bipolaron is formed, two electrons are removed from the $-\omega_0$ level (Fig. 18d). Thus, a positive bipolaron is expected to have the following intragap transitions:

- BP_1 transition: $-\omega_0$ level ← valence band
- BP_3 transition: $+\omega_0$ level ← valence band

The transition from the $-\omega_0$ level to the $+\omega_0$ level is missing, because the $-\omega_0$ level is unoccupied. When a negative bipolaron is formed, two electrons are added to the $+\omega_0$ level and thus two transitions are again expected (Fig. 18e). Within the Fesser–Bishop–Campbell model, the subgap absorption due to the BP_1 transition is much stronger than that due to the BP_3 transition, because the BP_3 transition is symmetry forbidden. Quantitatively, the intensities of these subgap absorptions are given as a function of the ratio ω_0/Δ_0.

The dications of oligothiophenes up to nonamer and oligophenylenevinylenes, and the dianions of oligophenyls and oligophenylenevinylenes give rise to one strong absorption band. These observations indicate that one subgap absorption is expected for a bipolaron in a nondegenerate polymer.

3.2.1.3. *Solitons*

Soliton excitations are possible only in degenerate polymers such as *trans*-polyacetylene. For a neutral soliton, a nonbonding electronic level is occupied by one electron. Thus, a neutral soliton is expected to have a single intragap transition (Fig. 18f):

- S transition: soliton nonbonding level ← valence band, and conduction band ← soliton nonbonding level

When a positive soliton is formed, one electron is removed from the soliton nonbonding level. In this case, one transition is also expected (Fig. 18g). When a negative soliton is formed, one electron is added to the soliton nonbonding orbital; thus, one transition is again expected (Fig. 18h). Each of α,ω-diphenyloligoenyl anions that are model compounds of a negative soliton gives rise to one absorption band, as described in the previous section. Thus, a single subgap absorption is expected for solitons.

Shimoi, Abe, and Harigaya [135] and Shimoi and Abe [136] calculated the optical absorption spectra associated with a polaron and a bipolaron by using a Peierls–Hubbard Hamiltonian with electron–phonon coupling and electron–electron interaction terms. According to their calculations, a polaron gives rise to two subgap absorption bands and a bipolaron gives rise to a single subgap absorption band. Essentially, their results are consistent with those obtained by the Fesser–Bishop–Campbell model.

3.2.2. *Polythiophenes*

As a typical example of nondegenerate polymers, the optical absorption spectrum of neutral polythiophene [137] is shown in Figure 19. The bandgap of polythiophene is estimated to be 1.94 eV from the onset of the observed absorption. The maximum absorption in substituted polythiophenes depends on the kind of substituents. Regioregular poly(3-alkylthiophene)s have been synthesized by head-to-tail coupling of 3-alkylthiophene [142, 143]. The absorption spectra of regioregular poly(3-alkylthiophene)s show distinct vibrational progressions, although those of regiorandom polymers show no progressions [142, 143]. These observations indicate that the structures of these polymers are homogeneous. Fluorescence is observed for polythiophenes. The light-emitting diodes fabricated with various types of substituted polythiophenes show colors ranging from blue to near-infrared [144].

The doping- and photoinduced absorption spectra of polythiophene, substituted polythiophenes, and their composites have been reported [145–166]. Let us discuss the subgap absorptions due to charged excitations in unsubstituted polythiophene. The optical absorption spectrum of BF_4^--doped polythiophene [42, 46] and the photoinduced absorption spectrum of polythiophene [145] are shown in Figure 20. In the spectrum of BF_4^--doped polythiophene (Fig. 20a), doping-induced bands are observed at 0.73 and 1.68 eV, which are located below the gap edge, 1.94 eV. The 0.73-

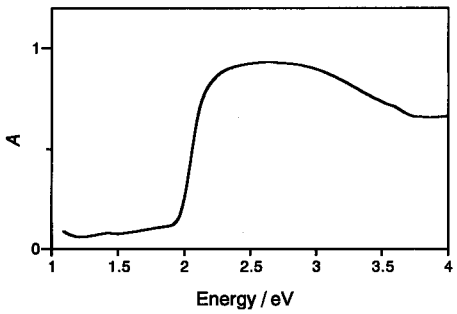

Fig. 19. Optical absorption spectrum of a polythiophene film.

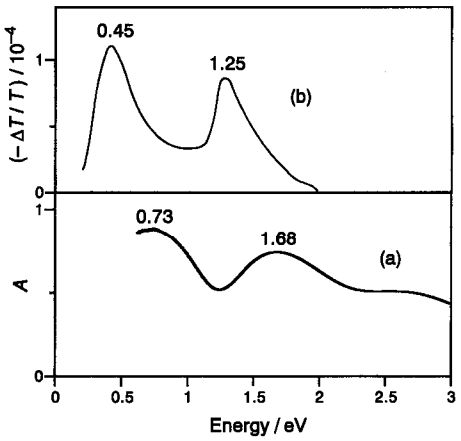

Fig. 20. (a) Optical absorption spectrum of a BF_4^--doped polythiophene film (room temperature) and (b) photoinduced absorption spectrum of a polythiophene film (20 K).

and 1.68-eV absorption bands are assigned to the P_1 and P_2 transitions expected for a positive polaron. Thus, it can be concluded that positive polarons are formed on BF_4^--doping (p-type doping). The electronic absorption spectra of ClO_4^--doped polythiophene at various dopant content have been reported by Chung et al. [146] and Kaneto et al. [147]. The band positions depend slightly on the dopant content. At the maximum doping level, the two-band feature disappears and absorption extending to the infrared region is observed. This result is reminiscent of free carrier absorption. The optical absorption spectra of photogenerated carriers in conjugated polymers can be measured by the steady-sate method, because the lifetimes of the photogenerated carriers are in the range from micro- to milliseconds. In the photoinduced difference absorption spectrum of polythiophene, two broad bands are observed at 0.45 and 1.25 eV as shown in Figure 20b [145]. The observed photon energy of each photoinduced absorption band is lower than that of the doping-induced band, as clearly shown in Figure 20. The 0.45- and 1.25-eV bands are assigned to the P_1 and P_2 transitions of polarons [129]. Thus, the charge separation induced by photoirradiation can result in the formation of a positive polaron and a negative polaron. Lane et al. [129] reported that the photoinduced absorption spectrum of a polythiophene film annealed at 573 K for 30 min is dominated by a single band at 0.9 eV (Table XV). This absorption band is assigned to the BP_1 transition of bipolarons [129].

The assignments of the doping- and photoinduced absorption bands of polythiophene, substituted polythiophenes, and their composites are listed in Table XVI. Note that the two-band feature attributed previously to bipolarons has been newly ascribed to polarons. In addition to the previously described subgap absorption bands of polythiophene, additional bands have been observed in the range between 1.8 and 1.96 eV by modulation and time-resolved measurements [145, 148, 149, 166]. These bands have been ascribed to a triplet exciton [145, 148]. The observed positions, 1.96 eV, are higher than the position 1.54 eV [62] of the $T_n \leftarrow T_1$ absorption of undecamer in a CH_2Cl_2 solution. The positions of the bands attributed to triplet excitons in substituted polythiophenes are sensitive to the substituents and solvents, as shown in Table XVI. The photoinduced band observed at 1.8 eV is assigned to a polaron pair [149, 166]. In the composite of a conjugated polymer and buckminsterfullerene C_{60}, C_{60} acts as a strong electron acceptor upon photoirradiation [12, 161, 165]. Photoluminescence and electroluminescence are quenched upon doping by a small amount of C_{60}, whereas photoconductivity is enhanced [12, 161, 165]. In a polythiophene–C_{60} composite, charge separation occurs efficiently. Thus the intensities of the subgap absorptions due to polarons become strong. Friend and co-workers [167–169] reported *in situ* voltage-induced electronic absorption spectra of field-effect transistors fabricated with poly(3-hexylthiophene). They observed the absorption bands due to injected carriers in the electronic devices.

3.2.3. *Polyarylenevinylenes*

Poly(*p*-phenylenevinylene) derivatives are promising candidates for the active layer of polymer light-emitting diodes. Thus, various types of substituted poly(*p*-phenylenevinylene)s have been synthesized. Whereas these derivatives are soluble in organic solvents, a high-quality thin film of these polymers can be formed. The optical properties of these polymers have been reviewed previously [8, 169]. The electroluminescence spectrum of the device fabricated with a conjugated polymer is almost the same as that of the photoluminescence spectrum of the thin film of the polymer. The peaks in photoluminescence spectra are compiled in Table XVII [170, 171].

Doping- and photoinduced electronic absorptions in poly(*p*-phenylenevinylene), substituted poly(*p*-phenylenevinylene)s, and their composites, have been reported [88, 131, 132, 160, 164–166, 172–181]. In the optical absorption spectrum of ClO_4^--doped poly(*p*-phenylenevinylene), doping-induced subgap absorption bands are observed at 0.9 and 2.3 eV (Table XV). These two bands are assigned to the P_1 and P_3 transitions of a polaron. Thus, positive polarons are formed upon ClO_4^- doping (p-type doping). On the other hand, a single band is observed at 1.55 eV in the absorption spectrum of Na-doped poly(*p*-phenylenevinylene) (Table XV). According to a Raman study [88] of Na-doped poly(*p*-phenylenevinylene), both negative polarons and negative bipolarons are generated upon Na doping. The observed 1.55-eV bands are overlapped by the absorptions of negative polarons and negative bipolarons [88]. The photoinduced bands observed at 0.6 and 1.6 eV (Table XV) are also assigned to the P_1 and P_3 transitions of polarons. Thus the charge separation induced by photoirradiation can result in the formation of a positive polaron and a negative polaron, as is the case in polythiophene.

The assignments of doping- and photoinduced absorption bands of polyarylenevinylenes and their composites are listed in Table XVIII. Note again that the two-band feature is assigned to polarons in this review, in contrast to the previous assignments that

Table XVI. Assignments of the Doping-Induced and Photoinduced Absorption Bands of Polythiophenes and Their Composites

Polymer[a]	Method[b]	Band (eV)	State/solvent	Species	Ref.
PT	PI	1.95	Film	Triplet exciton	[145]
		1.96	Film	Triplet exciton	[148]
		1.8	Film	Polaron pair	[166]
PMT	DI	0.65, 1.6	Film	Polaron	[154]
PET	DI	0.7, 1.6	Film	Polaron	[151]
PHT	DI	0.45, 1.65	Film	Polaron	[155]
	PI	0.35, 1.3	Film	Polaron	[155]
	VI	0.3–0.35, 1.35, 1.75	Device	Polaron	[169]
POT	DI	0.6, 1.6	Film	Polaron	[160]
	PI	<0.2, 1.25	Film	Polaron	[160, 162]
	PI	1.05	Film	Triplet exciton	[160]
PDT	PI	<0.35, 1.25	Film	Polaron	[158]
	PI	1.75	Film	—	[158]
	PI	0.55, 1.55	Chloroform	Polaron	[158]
	PI	2.1	Chloroform	—	[158]
PDDT	PI	1	Film	Triplet exciton	[156]
PMBET	PI	1.1	Film	Triplet exciton	[164]
	PI	1.24	Film	Polaron	[164]
	PI	<0.64, 1.47	1,2-Dichlorobenzene	Polaron	[163]
	PI	1.47	1,2-Dichlorobenzene	Triplet exciton	[163]
	PI	1.5	*p*-Xylene	Triplet exciton	[163]
POT–C_{60}	PI	1.45	Film	Polaron	[160]
PMBET–C_{60}	PI	<0.7, 1.26	Film	Polaron	[164]
	PI	<0.64, 1.47	1,2-Dichlorobenzene	Polaron	[163]
PMBET–A	PI	<0.7, 1.26	Film	Polaron	[164]

[a]PT, polythiophene; PMT, poly(3-methylthiophene); PHT, poly(3-hexylthiophene); POT, poly(3-octylthiophene); PDT, poly(3-decylthiophene); PDDT, poly(3-dodecylthiophene); PMBET, poly(3-(2-(3-methylbutoxy)ethyl)thiophene); A, tetracyano-*p*-quinodimethane and its derivatives.

[b]DI, doping induced; PI, photoinduced: VI, voltage induced.

Table XVII. Maximum Wavelength of Photoluminescence in Poly(*p*-phenylenevinylene) Derivatives

Polymer[a]	Wavelength (nm)	State/solvent	Ref.
PPV	550	Film	[170]
BuEH-PPV	560	Film	[8]
DOO-PPV	582	Film	[171]
MEH-PPV	555	Toluene	[170]
	630	Film	[170]
CN-PPV	555	Toluene	[170]
	690	Film	[170]

[a]PPV, poly(1,4-phenylenevinylene); BuEH-PPV, poly(2-butyl-5-(2′-ethylhexyl)-1,4-phenylenevinylene); DOO-PPV, poly(2,5-dioctoxy-1,4-phenylenevinylene); MEH-PPV, poly(2-methoxy-5-(2′-ethylhexyloxy)-1,4-phenylenevinylene).

the two-band feature is due to bipolarons. In addition to these photoinduced absorption bands, additional bands have been observed at 1.45 and 1.36 eV [132, 176]. These bands have been ascribed to triplet excitons [132, 176], because a single absorption attributed to the $T_n \leftarrow T_1$ transition is observed between 1.61 and 2.12 eV for each oligomer [86]; 4Bu-PV6 gives rise to the absorption due to the $T_n \leftarrow T_1$ transition at 1.61 eV. Brown et al. [180] reported the *in situ* voltage-induced absorption spectra of electroluminescent devices (polymer light-emitting diodes) fabricated with poly(*p*-phenylenevinylene). These *in situ* absorption measurements are useful in studying the mechanism of electroluminescence in the devices, because injected carriers cannot be detected by fluorescence spectroscopy, but by absorption spectroscopy.

3.2.4. *Polyacetylene*

In the optical absorption spectrum of AsF_6^--doped *trans*-polyacetylene, a single band is observed at 0.7 eV [122] (Table XV). This is half the bandgap (1.4 eV) [122] of *trans*-polyacetylene. This subgap absorption band is assigned to the S transition of a positive soliton generated by p-type doping, because the energy of the S transition is half the bandgap (Fig. 17g). The subgap absorption at 0.7 eV in Na-doped *trans*-polyacetylene is also attributed to the S transition of a negative soliton. Photoinduced electronic absorptions in

Table XVIII. Assignments of the Doping-Induced and Photoinduced Bands of Poly(arylenevinylene)s and Their Composites

Polymer[a]	Method[b]	Band (eV)	State/solvent	Species	Ref.
PPV	PI	1.45	Film	Triplet exciton	[132]
	PI	1.36	Film	Triplet exciton	[176]
	VI	0.65, 1.55	Device	Polaron	[180]
	VI	1.37	Device	Triplet exciton	[180]
DMO-PPV	DI	0.68, 1.76	Film	Polaron	[173]
	PI	0.45, 1.35	Film	Polaron	[173]
	PI	0.68, 1.80	Film	Polaron	[175]
	PI	1.35	Film	Triplet exciton	[175]
DOO-PPV	DI	0.60, 1.55	Film	Polaron	[173]
	PI	0.37, 1.36	Film	Polaron	[173]
	PI	0.35, 1.3	Film	Polaron	[174]
	PI	1.36	Film	Triplet exciton	[174]
MEH-PPV	DI	0.57, 1.59	Film	Polaron	[173]
	PI	0.43, 1.36	Film	Polaron	[173]
	PI	1.34	Film	Triplet exciton	[164]
BCHA-PPV	PI	1.47	Film	Triplet exciton	[178]
	PI	1.5	*p*-xylene	Triplet exciton	[178]
MEH-PPV/C_{60}	PI	<0.7, 1.5–2.0	Film	Polaron	[164]
	PI	1.34	Film	Triplet exciton	[164]
DOO-PPV/C_{60}	PI	0.45, 1.4	Film	Polaron	[166]
	PI	0.4, 1.8	Film	Polaron pair	[166]
BCHA-PPV/C_{60}	PI	0.43, 1.47	Film	Polaron	[178]
PBTV	PI	0.55, 1.1	Chloroform	Polaron	[159]

[a]PPV, poly(1,4-phenylenevinylene); DMO-PPV, poly(2,5-dimethoxy-1,4-phenylenevinylene); DHO, poly(2,5-dihexoxy-1,4-phenylenevinylene); DOO-PPV, poly(2,5-dioctoxy-1,4-phenylenevinylene); MEH-PPV, poly(2-methoxy-5-(2′-ethylhexyloxy)-1,4-phenylenevinylene); BCHA-PPV, poly(bis-2,5-*epi*-cholestanoxy-1,4-phenylenevinylene); PBTV, poly(3-butyl-2,5-thienylenevinylene).

[b]Abbreviations as cited in footnote b of Table XVI.

trans-polyacetylene have been reported [181–185]. Photoinduced bands are observed at 0.5 and 1.35 eV. The band at 0.5 eV has been ascribed to charged solitons [182, 183], because the position at 0.5 eV is similar to that of the 0.7-eV band attributed to a positive soliton in acceptor-doped *trans*-polyacetylene. Orenstein and Baker [181] showed that the band at 1.35 eV can be correlated with the $T_n \leftarrow T_1$ transitions of oligoenes. A triplet exciton is viewed as a neutral soliton pair. Levey et al. [186] ascribed the 1.35-eV band to a neutral soliton on the basis of the results of light-induced ESR measurements. Wei et al. [174] confirmed this assignment by absorption detected magnetic resonance measurements. Burroughes et al. [187] reported the voltage-induced electronic absorption spectra of field-effect transistors fabricated with Durham polyacetylene; they observed a voltage-induced absorption band at 0.55 eV, which is assigned to injected charged solitons.

4. CONCLUDING REMARKS

The optical absorption and emission spectra of conjugated polymers and oligomers have been reviewed. The optical bandgaps of the conjugated polymers that are organic semiconductors range from 1 to 3.5 eV. The photoluminescence spectra of conjugated polymers and oligomers are useful in designing electroluminescent devices (light-emitting diodes) fabricated with conjugated polymers. The subgap absorptions induced by chemical doping or photoirradiation are associated with self-localized excitations (solitons, polarons, bipolarons, and excitons) in conjugated polymers. Charged solitons, polarons, and bipolarons are charge carriers in conjugated polymers. Doping- and photoinduced absorptions have been studied on the basis of the absorption spectra of model compounds: the radical ions, the divalent ions, the anions, and the T_1 states of various oligomers. The two subgap absorptions are expected for a polaron and a single subgap absorption is expected for a bipolaron in nondegenerate polymers. In most nondegenerate polymers, such as polythiophenes, poly(*p*-phenylene)s, polypyrrole, poly(*p*-phenylenevinylene)s, and poly(2,5-thienylenevinylene)s, the doping- and photoinduced two-band features are observed and attributed to polarons. Thus polarons are the major carriers generated by chemical doping or photoirradiation.

Acknowledgments

The present work was supported in part by Toyota Physical and Chemical Research Institute, an International Joint Research

Grant from NEDO, and a grant-in-aid for scientific research on priority areas, "Molecular Physical Chemistry," from the Ministry of Education, Science, Sports, and Culture.

REFERENCES

1. H. Shirakawa, E. J. Louis, A. G. MacDiarmid, C. K. Chiang, and A. J. Heeger, *J. Chem. Soc., Chem. Commun.* 1977, 578 (1977).
2. H. Kiess, Ed., "Conjugated Conducting Polymers." Springer-Verlag, Berlin, 1992.
3. H. S. Nalwa, Ed., "Organic Conductive Molecules and Polymers," Vols. 1–4. Wiley, New York, 1997.
4. A. Tsumura, H. Koezuka, and T. Ando, *Appl. Phys. Lett.* 49, 1210 (1986).
5. J. H. Burroughes, C. A. Jones, and R. H. Friend, *Nature* 335, 137 (1988).
6. G. Yu, J. Gao, J. C. Hummelen, F. Wudl, and A. J. Heeger, *Science* 270, 1789 (1995).
7. J. H. Burroughes, D. D. C. Bradley, A. R. Brown, R. N. Marks, K. Mackay, R. H. Friend, P. L. Burns, and A. B. Holmes, *Nature* 347, 539 (1990).
8. F. Hide, M. A. Díaz-García, B. J. Schwartz, and A. J. Heeger, *Acc. Chem. Res.* 30, 430 (1997).
9. S. Miyata and H. S. Nalwa, Eds., "Organic Electroluminescent Materials and Devices." Gordon and Breach, Amsterdam, 1997.
10. R. H. Friend, R. W. Gymer, A. B. Holmes, J. H. Burroughes, R. N. Marks, C. Taliani, D. D. C. Bradley, D. A. Dos Santos, J. L. Brédas, M. Lögdlund, and W. R. Salaneck, *Nature* 397, 121 (1999).
11. H. G. Kiess and G. Harbeke, in "Conjugated Conducting Polymers" (H. Kiess, Ed.), p. 184. Springer-Verlag, Berlin, 1992.
12. N. S. Sariciftci, L. Smilowitz, A. J. Heeger, and F. Wudl, *Science* 258, 1474 (1992).
13. H. Spreitzer, H. Becker, E. Kluge, W. Kreuder, H. Schenk, R. Demandt, and H. Schoo, *Adv. Mater.* 10, 1340 (1998).
14. W. P. Su, J. R. Schrieffer, and A. J. Heeger, *Phys. Rev. Lett.* 42, 1698 (1979); *Phys. Rev. B* 22, 2099 (1980).
15. W. P. Su and J. R. Schrieffer, *Proc. Natl. Acad. Sci. USA* 77, 5626 (1980).
16. S. A. Brazovskiĭ and N. N. Kirova, *Sov. Phys. JETP Lett.* 33, 4 (1981).
17. A. R. Bishop, D. K. Campbell, and K. Fesser, *Mol. Cryst. Liq. Cryst.* 77, 253 (1981).
18. J. L. Brédas, R. R. Chance, and R. Silbey, *Mol. Cryst. Liq. Cryst.* 77, 319 (1981).
19. L. Salem, "The Molecular Orbital Theory of Conjugated Systems." Benjamin, New York, 1966.
20. B. E. Kohler, in "Conjugated Polymers" (J. L. Brédas and R. Silbey, Eds.), pp. 405–434. Kluwer, Dordrecht, 1991.
21. C. R. Fincher, Jr., C.-E. Chen, A. J. Heeger, A. G. MacDiarmid, and J. B. Hasting, *Phys. Rev. Lett.* 48, 100 (1982).
22. C. S. Yannoni and T. C. Clarke, *Phys. Rev. Lett.* 51, 1191 (1983).
23. S. Hirata, H. Torii, and M. Tasumi, *J. Chem. Phys.* 103, 8964 (1995).
24. M. Ciofalo and G. L. Manna, *Chem. Phys. Lett.* 263, 73 (1996).
25. F. Martinez, R. Voelkel, D. Naegele, and H. Naarmann, *Mol. Cryst. Liq. Cryst.* 167, 227 (1989).
26. S. Hotta and K. Waragai, *J. Mater. Chem.* 1, 835 (1991).
27. W. ten Hoeve, H. Wynberg, E. E. Havinga, and E. W. Meijer, *J. Am. Chem. Soc.* 113, 5887 (1991).
28. J. Guay, P. Kasai, A. Diaz, R. Wu, J. M. Tour, and L. H. Dao, *Chem. Mater.* 4, 1097 (1992).
29. A. Yassar, D. Delabouglise, M. Hmyene, B. Nessak, G. Horowitz, and F. Garnier, *Adv. Mater.* 4, 490 (1992).
30. P. Bäuerle, U. Segelbacher, K.-U. Gaudl, D. Huttenlocher, and M. Mehring, *Angew. Chem. Int. Ed. Engl.* 32, 76 (1993).
31. P. Bäuerle, U. Segelbacher, A. Maier, and M. Mehring, *J. Am. Chem. Soc.* 115, 10,217 (1993).
32. M. Sato and M. Hiroi, *Chem. Lett.* 1994, 985 (1994).
33. Y. Yu, E. Gunic, B. Zinger, and L. L. Miller, *J. Am. Chem. Soc.* 118, 1013 (1996).
34. H. Nakanishi, N. Sumi, Y. Aso, and T. Otsubo, *J. Org. Chem.* 63, 8632 (1998).
35. J. A. E. H. van Haare, E. E. Havinga, J. L. J. van Dongen, R. A. J. Janssen, J. Cornil, and J.-L. Brédas, *Chem. Eur. J.* 4, 1509 (1998).
36. Y. Kanemitsu, K. Suzuki, Y. Masumoto, Y. Tomiuchi, Y. Shiraishi, and M. Kuroda, *Phys. Rev. B* 50, 2301 (1994).
37. R. S. Becker, J. S. de Melo, A. L. Maçanita, and F. Elisei, *J. Phys. Chem.* 100, 18,683 (1996).
38. D. Fichou, G. Horowitz, B. Xu, and F. Garnier, *Synth. Met.* 39, 243 (1990).
39. J. V. Caspar, V. Ramamurthy, and D. R. Corbin, *J. Am. Chem. Soc.* 113, 600 (1991).
40. M. G. Hill, K. R. Mann, L. L. Miller, and J.-F. Penneau, *J. Am. Chem. Soc.* 114, 2728 (1992).
41. M. G. Hill, J.-F. Penneau, B. Zinger, K. R. Mann, and L. L. Miller, *Chem. Mater.* 4, 1106 (1992).
42. Y. Furukawa, N. Yokonuma, M. Tasumi, M. Kuroda, and J. Nakayama, *Mol. Cryst. Liq. Cryst.* 256, 113 (1994).
43. J. Poplawski, E. Ehrenfreund, J. Cornil, J. L. Brédas, R. Pugh, M. Ibrahim, and A. J. Frank, *Mol. Cryst. Liq. Cryst.* 256, 407 (1994).
44. R. A. J. Janssen, D. Moses, and N. S. Sariciftci, *J. Chem. Phys.* 101, 9519 (1994).
45. B. Nessakh, G. Horowitz, F. Garnier, F. Deloffre, P. Srivastava, and A. Yassar, *J. Electroanal. Chem.* 399, 97 (1995).
46. N. Yokonuma, Y. Furukawa, M. Tasumi, M. Kuroda, and J. Nakayama, *Chem. Phys. Lett.* 255, 431 (1996).
47. D. Okamura, Y. Furukawa, N. Katano, and J. Nakayama, unpublished data.
48. J. Cornil, D. Beljonne, and J. L. Brédas, *J. Chem. Phys.* 103, 842 (1995).
49. Y. Furukawa, *J. Phys. Chem.* 100, 15,644 (1996).
50. Y. Furukawa, in "Primary Photoexcitations in Conjugated Polymers: Molecular Exciton versus Semiconductor Band Model" (N. S. Sariciftci, Ed.), pp. 496–523. World Scientific, Singapore, 1997.
51. A. J. W. Tol, *Chem. Phys.* 208, 73 (1996).
52. S. Irle and H. Lischka, *J. Chem. Phys.* 107, 3021 (1997).
53. R. A. J. Janssen, in "Primary Photoexcitations in Conjugated Polymers: Molecular Exciton versus Semiconductor Band Model" (N. S. Sariciftci, Ed.), pp. 524–558. World Scientific, Singapore, 1997.
54. D. Birnbaum and B. E. Kohler, *J. Chem. Phys.* 90, 3506 (1989).
55. D. Birnbaum and B. E. Kohler, *J. Chem. Phys.* 95, 4783 (1991).
56. D. Birnbaum, D. Fichou, and B. E. Kohler, *J. Chem. Phys.* 96, 165 (1992).
57. N. Periasamy, R. Danieli, G. Ruani, R. Zamboni, and C. Taliani, *Phys. Rev. Lett.* 68, 919 (1992).
58. F. Charra, D. Fichou, J.-M. Nunzi, and N. Pfeffer, *Chem. Phys. Lett.* 192, 566 (1992).
59. D. V. Lap, D. Grebner, S. Rentsch, and H. Naarmann, *Chem. Phys. Lett.* 211, 135 (1993).
60. D. Grebner, M. Helbig, and S. Rentsh, *J. Phys. Chem.* 99, 16,991 (1995).
61. J. P. Reyftmann, J. Kagan, R. Santus, and P. Morliere, *Photochem. Photobiol.* 41, 1 (1985).
62. R. A. J. Janssen, L. Smilowitz, N. S. Sariciftci, and D. Moses, *J. Chem. Phys.* 101, 1787 (1994).
63. F. Negri and M. Z. Zgierski, *J. Chem. Phys.* 100, 2571 (1994).
64. R. Colditz, D. Grebner, M. Helbig, and S. Rentsch, *Chem. Phys.* 201, 309 (1995).
65. M. Belletête, N. D. Césare, M. Leclerc, and G. Durocher, *Chem. Phys. Lett.* 250, 31 (1996).
66. A. E. Gillam and D. H. Hey, *J. Chem. Soc.* 1170 (1939).
67. J. Dale, *Acta Chem. Scand.* 11, 650 (1957).
68. H. Gregorius, W. Heitz, and K. Müllen, *Adv. Mater.* 5, 279 (1993).

69. P. Balk, G. J. Hoijtink, and J. W. H. Schreurs, *Rec. Trav. Chim.* 76, 813 (1957).
70. K. H. J. Buschow, J. Dieleman, and G. J. Hoijtink, *J. Chem. Phys.* 42, 1993 (1965).
71. J. Sagiv, A. Yogev, and Y. Mazur, *J. Am. Chem. Soc.* 99, 6861 (1977).
72. H. Hiratsuka, Y. Hatano, Y. Tanizaki, and Y. Mori, *J. Chem. Soc. Faraday Trans.* 2 81, 1653 (1985).
73. Y. Furukawa, H. Ohtsuka, and M. Tasumi, *Synth. Met.* 55, 516 (1993).
74. R. K. Khanna, Y. M. Jiang, B. Srinivas, C. B. Smithhart, and D. L. Wertz, *Chem. Mater.* 5, 1792 (1993).
75. R. Zahradník and P. Cársky, *J. Phys. Chem.* 74, 1240 (1970).
76. M. Rubio, M. Merchán, E. Ortí, and B. O. Roos, *J. Phys. Chem.* 99, 14,980 (1995).
77. V. G. Drefahl, R. Kühmstedt, and H. Oswald, *Makromol. Chem.* 131, 89 (1970).
78. C. W. Spangler, T. J. Hall, L. S. Sapochak, and P.-K. Liu, *Polymer* 30, 1166 (1989).
79. C. W. Spangler and T. J. Hall, *Synth. Met.* 44, 85 (1991).
80. J. M. Oberski, A. Greiner, and H. Bässler, *Chem. Phys. Lett.* 184, 391 (1991).
81. R. Schenk, H. Gregorius, and K. Müllen, *Adv. Mater.* 3, 492 (1991).
82. R. Schenk, H. Gregorius, K. Meerholz, J. Heize, and K. Müllen, *J. Am. Chem. Soc.* 113, 2634 (1991).
83. A. Sakamoto, Y. Furukawa, and M. Tasumi, *J. Phys. Chem.* 96, 1490 (1992).
84. M. Deussen and H. Bässler, *Chem. Phys.* 164, 247 (1992).
85. A. Sakamoto, Y. Furukawa, and M. Tasumi, *J. Phys. Chem.* 96, 3870 (1992).
86. H. S. Woo, O. Lhost, S. C. Graham, D. D. C. Bradley, R. H. Friend, C. Quattrocchi, J. L. Brédas, R. Schenk, and K. Müllen, *Synth. Met.* 59, 13 (1993).
87. A. Sakamoto, Y. Furukawa, and M. Tasumi, *J. Phys. Chem.* 98, 4635 (1994).
88. Y. Furukawa, A. Sakamoto, and M. Tasumi, *Macromol. Symp.* 101, 95 (1996).
89. S. Karabunarliev, M. Baumgarten, N. Tyutyulkov, and K. Müllen, *J. Phys. Chem.* 98, 11,892 (1994).
90. J. Cornil, D. Beljonne, and J. L. Brédas, *J. Chem. Phys.* 103, 834 (1995).
91. A. Sakamoto, Y. Furukawa, and M. Tasumi, *J. Phys. Chem. B* 101, 1726 (1997).
92. W. G. Herkstroeter and D. S. McClure, *J. Am. Chem. Soc.* 90, 4522 (1968).
93. Z. G. Soos, S. Ramasesha, D. S. Galvão, and S. Etemad, *Phys. Rev. B* 47, 1742 (1993).
94. Z. Shuai, J. L. Brédas, and W. P. Su, *Chem. Phys. Lett.* 228, 301 (1994).
95. D. Beljonne, Z. Shuai, R. H. Friend, and J. L. Brédas, *J. Chem. Phys.* 102, 2042 (1995).
96. B. I. Greene, R. M. Hochstrasser, and R. B. Weisman, *Chem. Phys. Lett.* 62, 427 (1979).
97. L. Zechmeister, "Cis-Trans Isomeric Carotenoids, Vitamins A, and Arylpolyenes." Academic Press, New York, 1962.
98. B. S. Hudson, B. E. Kohler, and K. Schulten, *Excited States* 6, 1 (1982).
99. Y. Furukawa, in "The Chemistry of Dienes and Polyenes" (Z. Rappoport, Ed.), Vol. 1, pp. 149–172. Wiley, Chichester, 1997.
100. F. Sondheimer, D. A. Ben-Efram, and R. Wolovsky, *J. Am. Chem. Soc.* 83, 1675 (1961).
101. W. F. Forbes, R. Shilton, and A. Balasubramanian, *J. Org. Chem.* 29, 3527 (1964).
102. C. W. Spangler and D. A. Little, *J. Chem. Soc. Perkin Trans. 1* 1982, 2379 (1982).
103. P. Nayler and M. C. Whiting, *J. Chem. Soc.* 3037 (1955).
104. C. W. Spangler and R. A. Rathunde, *J. Chem. Soc., Chem. Commun.* 1989, 26 (1989).
105. K. Knoll and R. R. Schrock, *J. Am. Chem. Soc.* 111, 7989 (1989).
106. K. W. Hausser, R. Kuhn, A. Smakula, and K. H. Kreuchen, *Z. Phys. Chem.* B29, 363 (1935).
107. K. W. Hausser, R. Kuhn, and A. Smakula, *Z. Phys. Chem.* B29, 384 (1935).
108. C. W. Spangler, P.-K. Liu, A. A. Dembek, and K. O. Havelka, *J. Chem. Soc. Perkin Trans. 1* 1991, 799 (1991).
109. G. J. Hoijtink and P. H. van der Meij, *Z. Phys. Chem. Neue Folge* 20, 1 (1959).
110. H. M. Parkes and R. N. Young, *J. Chem. Phys. Perkin 2* 1980, 1137 (1980).
111. L. M. Tolbert and M. E. Ogle, *Synth. Met.* 41, 1389 (1991).
112. T. Yamabe, K. Akagi, T. Matsui, K. Fukui, and H. Shirakawa, *J. Phys. Chem.* 86, 2365 (1982).
113. Z. G. Soos and L. R. Ducasse, *J. Chem. Phys.* 78, 4092 (1983).
114. T. Bally, K. Roth, W. Tang, R. R. Schrock, K. Knoll, and L. Y. Park, *J. Am. Chem. Soc.* 114, 2440 (1992).
115. Y. Kawashima, K. Nakayama, H. Nakano, and K. Hirao, *Chem. Phys. Lett.* 267, 82 (1997).
116. P. Mathis and J. Kleo, *Photochem. Photobiol.* 18, 343 (1973).
117. F. W. Langkilde, R. Wilbrandt, and N.-H. Jensen, *Chem. Phys. Lett.* 111, 372 (1984).
118. N. S. Sariciftci, Ed., "Primary Photoexcitations in Conjugated Polymers: Molecular Exciton versus Semiconductor Band Model." World Scientific, Singapore, 1997.
119. J. L. Brédas and G. B. Street, *Acc. Chem. Res.* 18, 309 (1985).
120. M. Tabata, M. Satoh, K. Kaneto, and K. Yoshino, *J. Phys. Soc. Jpn.* 55, 1305 (1986).
121. S. Yamada, S. Tokito, T. Tsutsui, and S. Saito, *J. Chem. Soc., Chem. Commun.* 1987, 1448 (1987).
122. A. O. Patil, A. J. Heeger, and F. Wudl, *Chem. Rev.* 88, 183 (1988).
123. R. P. McCall, J. M. Ginder, J. M. Leng, H. J. Ye, S. K. Manohar, J. G. Masters, G. E. Asturias, A. G. MacDiarmid, and A. J. Epstein, *Phys. Rev. B* 41, 5202 (1990).
124. A. J. Epstein, R. P. McCall, J. M. Ginder, and A. G. MacDiarmid, in "Spectroscopy of Advanced Materials" (R. J. H. Clark and R. E. Hester, Eds.), pp. 355–396. Wiley, New York, 1991.
125. K. Pichler, D. A. Halliday, D. D. C. Bradley, P. L. Burn, R. H. Friend, and A. B. Holmes, *J. Phys. Condens. Matter* 5, 7155 (1993).
126. A. J. Heeger, S. Kievelson, J. R. Schrieffer, and W.-P. Su, *Rev. Mod. Phys.* 60, 781 (1988).
127. G. B. Blanchet, C. R. Fincher, T. C. Chung, and A. J. Heeger, *Phys. Rev. Lett.* 50, 1938 (1983).
128. K. Kaneto, S. Ura, K. Yoshino, and Y. Inuishi, *Jpn. J. Appl. Phys.* 23, L189 (1984).
129. P. A. Lane, X. Wei, and Z. V. Vardeny, *Phys. Rev. Lett.* 77, 1544 (1996).
130. M. Satoh, M. Tabata, F. Uesugi, K. Kaneto, and K. Yoshino, *Synth. Met.* 17, 595 (1987).
131. D. D. C. Bradley, G. P. Evans, and R. H. Friend, *Synth. Met.* 17, 651 (1987).
132. D. D. C. Bradley, N. F. Colaneri, and R. H. Friend, *Synth. Met.* 29, E121 (1989).
133. A. J. Brassett, N. F. Colaneri, D. D. C. Bradley, R. A. Lawrence, R. H. Friend, H. Murata, S. Tokito, T. Tsutsui, and S. Saito, *Phys. Rev. B* 41, 10,586 (1990).
134. Y. Furukawa, *Synth. Met.* 69, 629 (1995).
135. Y. Shimoi, S. Abe, and K. Harigaya, *Mol. Cryst. Liq. Cryst.* 267, 329 (1995).
136. Y. Shimoi and S. Abe, *Synth. Met.* 78, 219 (1996).
137. Y. Furukawa, *J. Phys. Chem.* 100, 15,644 (1996).
138. P. A. Lane and Z. V. Vardeny, in "Primary Photoexcitations in Conjugated Polymers: Molecular Exciton versus Semiconductor Band Model" (N. S. Sariciftci, Ed.), pp. 292–317. World Scientific, Singapore, 1997.
139. R. H. Friend, D. D. C. Bradley, and P. D. Townsend, *J. Phys. D: Appl. Phys.* 20, 1367 (1987).
140. T. Kobayashi, Ed., "Relaxation in Polymers." World Scientific, Singapore, 1993.

141. K. Fesser, A. R. Bishop, and D. K. Campbell, *Phys. Rev. B* 27, 4804 (1983).
142. R. D. McCullough, R. D. Lowe, M. Jayaraman, and D. L. Anderson, *J. Org. Chem.* 58, 904 (1993).
143. T.-A. Chen, X. Wu, and R. D. Rieke, *J. Am. Chem. Soc.* 117, 233 (1995).
144. M. Berggren, O. Inganäs, G. Gustafsson, J. Rasmusson, M. R. Anderson, T. Hjertberg, and O. Wennerström, *Nature* 372, 444 (1994).
145. Z. Vardeny, E. Ehrenfreund, O. Brafman, M. Nowak, H. Schaffer, A. J. Heeger, and F. Wudl, *Phys. Rev. Lett.* 56, 671 (1986).
146. T.-C. Chung, J. H. Kaufman, A. J. Heeger, and F. Wudl, *Phys. Rev. B* 30, 702 (1984).
147. K. Kaneto, S. Hayashi, S. Ura, and K. Yoshino, *J. Phys. Soc. Jpn.* 54, 1146 (1985).
148. K. Kaneto, Y. Kohno, and K. Yoshino, *Solid State Commun.* 51, 267 (1984).
149. G. S. Kanner, X. Wei, B. C. Hess, L. R. Chen, and Z. V. Vardeny, *Phys. Rev. Lett.* 69, 538 (1992).
150. G. Harbeke, E. Meier, W. Kobel, M. Egli, H. Kiess, and E. Tosatti, *Solid State Commun.* 55, 419 (1985).
151. M. Sato, S. Tanaka, and K. Kaeriyama, *Synth. Met.* 14, 279 (1986).
152. Y. H. Kim, S. Hotta, and A. J. Heeger, *Phys. Rev. B* 36, 7486 (1987).
153. K. Kaneto, F. Uesugi, and K. Yoshino, *Solid State Commun.* 1987, 64, 1195 (1987).
154. N. Colaneri, M. Nowak, D. Spiegel, S. Hotta, and A. J. Heeger, *Phys. Rev. B* 36, 7964 (1987).
155. Y. H. Kim, D. Spiegel, S. Hotta, and A. J. Heeger, *Phys. Rev. B* 38, 5490 (1988).
156. J. Rühe, N. F. Colaneri, D. D. C. Bradley, R. H. Friend, and G. Wegner, *J. Phys. Condens. Matter* 2, 5465 (1990).
157. Z. W. Sun and A. J. Frank, *J. Chem. Phys.* 94, 4600 (1991).
158. C. Botta, S. Luzzati, R. Tubino, and A. Borghesi, *Phys. Rev. B* 46, 13,008 (1992).
159. C. Botta, S. Luzzati, R. Tubino, D. D. C. Bradley, and R. H. Friend, *Phys. Rev. B* 48, 14,809 (1993).
160. L. Smilowitz, N. S. Sariciftci, R. Wu, C. Gettinger, A. J. Heeger, and F. Wudl, *Phys. Rev. B* 47, 13,835 (1993).
161. K. Yoshino, T. Akashi, K. Yoshimoto, M. Yoshida, S. Morita, and A. A. Zakhidov, *Mol. Cryst. Liq. Cryst.* 256, 343 (1994).
162. K. Lee, R. A. J. Janssen, N. S. Sariciftci, and A. J. Heeger, *Phys. Rev. B* 49, 5781 (1994).
163. R. A. J. Janssen, N. S. Sariciftci, and A. J. Heeger, *J. Chem. Phys.* 100, 8641 (1994).
164. R. A. Janssen, M. P. T. Christiaans, C. Hare, N. Martin, N. S. Sariciftci, A. J. Heeger, and F. Wudl, *J. Chem. Phys.* 103, 8840 (1995).
165. N. S. Sariciftci, *Prog. Quant. Electron.* 19, 131 (1995).
166. P. A. Lane, X. Wei, and Z. V. Vardeny, *Phys. Rev. B* 56, 4626 (1997).
167. K. E. Ziemelis, A. T. Hussain, D. D. C. Bradley, R. H. Friend, J. Rühe, and G. Wegner, *Phys. Rev. Lett.* 66, 2231 (1991).
168. P. J. Brown, H. Sirringhaus, and R. H. Friend, *Synth. Met.* 101, 557 (1999).
169. H. Sirringhaus, P. J. Brown, R. H. Friend, M. M. Nielsen, K. Bechgaard, B. M. W. Langeveld-Voss, A. J. H. Spiering, R. A. J. Janssen, E. W. Meijer, P. Herwig, and D. M. de Leeuw, *Nature* 401, 685 (1999).
170. I. D. W. Samuel, G. Rumbles, and R. H. Friend, in "Primary Photoexcitations in Conjugated Polymers: Molecular Exciton versus Semiconductor Band Model" (N. S. Sariciftci, Ed.), pp. 140–173. World Scientific, Singapore, 1997.
171. T. Ohnishi, S. Doi, Y. Ysuchida, and T. Noguchi, in "Photonic and Optoelectronic Polymers" (S. A. Jenkhe and K. J. Wynne, Eds.), pp. 345–357. American Chemical Society, Washington, DC, 1997.
172. N. F. Colaneri, D. D. C. Bradley, R. H. Friend, P. L. Burn, A. B. Holmes, and C. W. Spangler, *Phys. Rev. B* 42, 11,670 (1990).
173. K. F. Voss, C. M. Foster, L. Smilowitz, D. Mihailovic, S. Askari, G. Srdanov, Z. Ni, S. Shi, A. J. Heeger, and F. Wudl, *Phys. Rev. B* 43, 5109 (1991).
174. X. Wei, B. C. Hess, Z. V. Vardeny, and F. Wudl, *Phys. Rev. Lett.* 68, 666 (1992).
175. H. S. Woo, S. C. Graham, D. A. Halliday, D. D. C. Bradley, R. H. Friend, P. L. Burn, and A. B. Holmes, *Phys. Rev. B* 46, 7379 (1992).
176. K. Pichler, D. A. Halliday, D. D. C. Bradley, P. L. Burn, R. H. Friend, and A. B. Holmes, *J. Phys. Condens. Matter* 5, 7155 (1993).
177. J. M. Leng, S. Jeglinski, X. Wei, R. E. Benner, Z. V. Vardeny, F. Guo, and S. Mazumdar, *Phys. Rev. Lett.* 72, 156 (1994).
178. R. A. J. Janssen, J. C. Hummelen, K. Lee, K. Pakbaz, N. S. Sariciftci, A. J. Heeger, and F. Wudl, *J. Chem. Phys.* 103, 788 (1995).
179. S. V. Frolov, P. A. Lane, M. Ozaki, K. Yoshino, and Z. V. Vardeny, *Chem. Phys. Lett.* 286, 21 (1998).
180. A. R. Brown, K. Pichler, N. C. Greenham, D. D. C. Bradley, R. H. Friend, and A. B. Holmes, *Chem. Phys. Lett.* 210, 61 (1993).
181. J. Orenstein and G. L. Baker, *Phys. Rev. Lett.* 49, 1043 (1982).
182. Z. Vardeny, J. Orenstein, and G. L. Baker, *Phys. Rev. Lett.* 50, 2032 (1983).
183. G. B. Blanchet, C. R. Fincher, T. C. Chung, and A. J. Heeger, *Phys. Rev. Lett.* 50, 1938 (1983).
184. Z. Vardeny, H. T. Grahn, L. Chen, and G. Leising, *Synth. Met.* 28, D167 (1989).
185. P. D. Townsend and R. H. Friend, *Phys. Rev. B* 40, 3112 (1989).
186. C. G. Levey, D. V. Lang, S. Etemad, G. L. Baker, and J. Orenstein, *Synth. Met.* 17, 569 (1987).
187. J. H. Burroughes, C. A. Jones, and R. H. Friend, *Nature* 335, 137 (1988).